Applied Mathematics and Computation 321 (2018) 401–421

Contents lists available at ScienceDirect

Applied Mathematics and Computation

journal homepage: www.elsevier.com/locate/amc

Numerical solution of generalized Black–Scholes model

S. Chandra Sekhara Rao*, Manisha

Department of Mathematics, Indian Institute of Technology Delhi, Hauz khas, New Delhi 110016, India

ARTICLE INFO

Keywords:
Degenerate parabolic partial differential equation
Generalized Black–Scholes model
HODIE (High-order difference approximation with identity expansions) scheme
Two-step backward differentiation formula

ABSTRACT

This paper presents a numerical scheme that approximates the option prices for different option styles, governed by the generalized Black–Scholes equation in its degenerate form. The proposed method uses the HODIE scheme in the spacial direction and the two-step backward differentiation formula in the temporal direction. It is proved that the method has second order convergence in space as well as in time. Numerical experiments validate the theoretical results.

1. Introduction

In a financial market, options, forwards, futures, etc. are among the derivative securities that are used in managing the risk and speculating the profit. There are different option styles like European, American, Bermudan, etc. These are the financial contracts in which the writer of the option sells the options to the holder and is paid a premium called option price. The premium is paid for conferring the right to buy (call option case) or sell (put option case) predefined quantities of one or more predetermined risky assets for a fixed price, the strike/exercise price. The option which is exercised on the date of expiry of the contract, called the maturity/expiration date, is the European option. And the option which can be exercised on or before the date of the maturity/expiry of the contract is the American option [1,2].

Let us assume one risk-free asset and one risky asset constitutes a market which is frictionless and without any arbitrage opportunity. The stock price (S) of the unit risky asset follows the following stochastic differential equation at time τ:

$$dS = (\mu - D)Sd\tau + \sigma SdW, \tag{1.1}$$

where μ is the drift, D is the dividend paid, σ is the market volatility and dW is the Wiener process. Now using Itô's lemma and eliminating the randomness in a complete market, we derive the famous Black–Scholes equation.

The Black–Scholes partial differential equation and its solution named as the Black–Scholes formula was derived by Fischer Black and Myron Scholes for theoretical valuation of option price in their seminal work [3]. The celebrated Black–Scholes model for evaluating European call option price $C(S, \tau)$ is given as

$$\frac{1}{2}\sigma^2 S^2 \frac{\partial^2 C}{\partial S^2} + (r - D)S\frac{\partial C}{\partial S} - rC = -\frac{\partial C}{\partial \tau}, \quad S > 0, \tau \in (0, T), \tag{1.2}$$

along with the final condition

$$C(S, T) = \max(S - K, 0), \qquad S \in [0, \infty), \tag{1.3}$$

* Corresponding author.
E-mail addresses: scsr@maths.iitd.ernet.in, scsr@maths.iitd.ac.in (S. Chandra Sekhara Rao), srivastava.manisha99@gmail.com (Manisha).

https://doi.org/10.1016/j.amc.2017.10.004
0096-3003/

where S is the asset price, τ is the current time, r is the risk free interest rate, T is the maturity date of contract and K is the strike price. The Black–Scholes equation, in which σ, r and D are constants, can be easily reduced to standard heat equation [3,4] and further solved to obtain the following closed form solution:

$$C(S,\tau) = S\exp(-D(T-\tau))N(d_1) - K\exp(-r(T-\tau))N(d_2), \tag{1.4a}$$

where

$$d_1 = \frac{\ln S - \ln K + \left(r - D + \frac{1}{2}\sigma^2\right)(T-\tau)}{\sigma\sqrt{T-\tau}}, \tag{1.4b}$$

$$d_2 = d_1 - \sigma\sqrt{T-\tau} \tag{1.4c}$$

and the cumulative standard normal distribution function $N(y)$ is defined as

$$N(y) = \frac{1}{\sqrt{2\pi}}\int_{-\infty}^{y}\exp\left(-\frac{1}{2}x^2\right)dx. \tag{1.4d}$$

The explicit formula for pricing options and warrants was also derived by Robert C. Merton in [5] under weaker assumptions.

When these parameters σ, r and D are dependent on stock price S and time variable τ, such simplification of the problem is not possible. Also the closed form solution of such generalized problem is not available.

The lattice methods and the finite difference methods were among the first methods for pricing derivative securities. Cox, Ross and Rubinstein, in [6], proposed the binomial option pricing formula for valuing options known as CRR model and proved that the binomial formula converges to the Black–Scholes formula in the limiting case. Earlier similar trinomial process was implemented to value American put option in [7]. Hull and White, in [8], generalized such lattice approach to option pricing.

The finite difference methods are the most common numerical approach to approximate the option price as the solution of Black–Scholes model, which avoid probability theory and stochastic methods. A detailed comparison of different approximation techniques for such price valuation where analytic solution does not exist was given in [9]. In [10], cubic B-spline was used to solve generalized Black–Scholes equation after transforming it to non-degenerate uniformly parabolic partial differential equation using logarithmic transform. [11–19] present various numerical schemes for option pricing using logarithmic transform of the Black–Scholes equation. Finite difference method which resolves the degeneracy effectively was given in [20]. But the problem considered was not dividend paying, the interest rate was only dependent on time and the scheme was of $O(h^2 + k)$ accuracy. Wang [21] and Valkov [22] used fitted finite volume method for spatial discretization for solving the degenerate Black–Scholes equation. Wang [21] developed a first order method after transforming the Dirichlet boundary condition of generalized Black–Scholes equation into homogeneous boundary condition and then writing the partial differential equation in its self-adjoint form. Recently, in [23], a penalized nonlinear Black–Scholes equation (with variable parameters) for evaluating European and American options was rewritten in the self-adjoint form and then numerically approximated. A second order fitted finite volume scheme was developed to numerically approximate the option price, the flux and the Delta of the option by deriving the superconvergence points in the subintervals of the primal mesh to form a dual mesh. Degeneracy issue of the considered problem was solved by refining the meshes locally near the point of degeneracy in order to maintain the second order accuracy in space. The temporal discretization was done using the Crank-Nicolson scheme along with Rannacher's technique. The Rannacher's technique, where the mesh size in time direction near $t = T$ was taken to be of order Δt^2, $(\Delta t = max_k|\Delta t_k|)$, was applied to ensure that the second order accuracy of Crank-Nicolson scheme was achieved.

In this paper, we have considered Black–Scholes equation governing four different option styles of European type with variable parameters. A numerical scheme which efficiently tackles the degeneracy concern of the Black–Scholes equation without performing logarithmic transform of the equation, without truncating the domain so as to exclude the point of degeneracy and without using nonuniform mesh near the point of degeneracy is presented. We implement simultaneous discretization in space and time using High-Order Difference approximation with Identity Expansion (HODIE) scheme in space direction [24] and two-step backward differentiation for temporal discretization. The simultaneous discretization in time and space using HODIE scheme in space direction was performed in [25,26]. Zhao, Davison and Corless [4] evaluated American options using a compact finite difference method, which is a special case of HODIE scheme, for inhomogeneous heat equation. We present a scheme which approximates option prices of different option styles like European call option, binary call option, long call butterfly spread option and also portfolio of options with butterfly spread delta function as the final condition, with corresponding changes in terminal and boundary conditions.

The paper is organized as follows: In Section 2, the generalized Black–Scholes partial differential equation with its boundary and terminal conditions is introduced. Some modifications are made so that the problem is in a form which can be dealt numerically. In Section 3, the numerical scheme is developed. In Section 4, convergence analysis of the scheme and the order of convergence of the solution are established. Section 5 gives the experimental results in accordance with theoretical claims of presented scheme. Finally Section 5 concludes the paper and discusses some additional merits and concerns of our scheme. Throughout the paper $\mathscr{C}$ denotes a generic positive constant.

2. The Black–Scholes partial differential equation

The generalized Black–Scholes model for evaluating European call option price $C(S, \tau)$ is

$$-\frac{\partial C}{\partial \tau} = \frac{1}{2}\sigma^2(S,\tau)S^2\frac{\partial^2 C}{\partial S^2} + (r(S,\tau) - D(S,\tau))S\frac{\partial C}{\partial S} - r(S,\tau)C, \quad S > 0, \tau \in (0,T), \tag{2.1a}$$

along with the final condition

$$C(S,T) = \max(S-K,0), \qquad S \in [0,\infty) \tag{2.1b}$$

and the boundary conditions

$$C(0,\tau) = 0, \tag{2.1c}$$

$$C(S,\tau) \to S, \quad \text{as } S \to \infty, \tag{2.1d}$$

where S, the asset price is working as the space variable, τ is the time variable, $\sigma(S, \tau)$ is the market volatility, $r(S, \tau)$ is the interest rate and $D(S, \tau)$ is the dividend yield of the asset. σ, r and D are assumed to be continuous and bounded functions of space and time variables within the contract period.

Eq. (2.1a) is a degenerate parabolic partial differential equation. The existence and uniqueness of the classical solution of the final value problem (2.1) can be ensured after the logarithmic transform of the space variable along with its conversion from final value problem to initial value problem [27].

The scheme, we are going to propose in this paper, not only solves vanilla options like European call and put but also easily deals with other exotic options and combination of options, for example binary call options, long call butterfly spread options and also portfolio of options with butterfly spread delta function as the final condition.

We consider cash-or-nothing binary call options. It satisfies the Black–Scholes Eq. (2.1a). As its name suggests, it has the following payoff at the maturity:

$$C(S,T) = \begin{cases} 0 & \text{for } S < K, \\ Q & \text{for } S \geq K. \end{cases}$$

The boundary conditions, which we can use in our computational domain are

$$C(0,\tau) = 0, \qquad \tau \in [0,T],$$

and

$$C(S,\tau) = Q\exp\left(-\int_\tau^T r(S,q)dq\right), \qquad \tau \in [0,T], \text{ for large } S.$$

A long call butterfly spread option consists of a combination of long and short selling of European call option over same underlying asset and with same maturity date. It has two options held under long position with strike price say K_1 and K_3 and two options held under short position with strike price say K_2. This also satisfies Black–Scholes Eq. (2.1a) with following payoff at the maturity:

$$C(S,T) = \max(S-K_1,0) - 2\max(S-K_2,0) + \max(S-K_3,0), \qquad S > 0$$

and the boundary conditions are

$$C(0,\tau) = 0, \qquad \tau \in [0,T],$$

$$C(S,\tau) = 0, \qquad \text{as } S \to \infty, \ \tau \in [0,T].$$

We also consider a portfolio of options with butterfly spread delta function as the final condition. It satisfies Black–Scholes Eq. (2.1a) with following payoff at the maturity:

$$C(S,T) = \begin{cases} 1 & \text{for } S \in (S1,S2), \\ -1 & \text{for } S \in (S2,S3), \\ 0 & \text{otherwise}, \end{cases}$$

and the boundary conditions are

$$C(0,\tau) = 0, \qquad \tau \in [0,T],$$

$$C(S,\tau) = 0, \qquad \text{as } S \to \infty, \ \tau \in [0,T]. \tag{2.2}$$

Observing the fact that the initial conditions of the above problems are not smooth, we need to ensure the convergence of the solution obtained from finite difference scheme ([28,29]). Hence we replace a small ϵ-neighborhood of the point of singularity by a ninth degree polynomial so that the payoff is a fourth order smooth function ([20]).

For the European option case, define a function $\psi(x)$ as

$$\psi(x) = \begin{cases} x & \text{for } x \geq \epsilon, \\ c_0 + c_1 x + c_2 x^2 + \ldots + c_9 x^9 & \text{for } -\epsilon < x < \epsilon, \\ 0 & \text{for } x \leq -\epsilon, \end{cases}$$

where $\epsilon > 0$ is a small constant and $c_i,\ i = 0, 1, \ldots, 9$ are the constant coefficients to be determined. Applying the following ten conditions on the function $\psi(x)$:

$$\psi(-\epsilon) = \psi'(-\epsilon) = \psi''(-\epsilon) = \psi'''(-\epsilon) = \psi^{(4)}(-\epsilon) = 0$$

$$\psi(\epsilon) = \epsilon, \psi'(\epsilon) = 1, \psi''(\epsilon) = \psi'''(\epsilon) = \psi^{(4)}(\epsilon) = 0$$

we can uniquely determine the unknown coefficients $c_i, i = 0, 1, \ldots, 9$ viz.:

$$c_0 = \frac{35}{256}\epsilon, \quad c_1 = \frac{1}{2}, \quad c_2 = \frac{35}{64\epsilon}, \quad c_4 = -\frac{35}{128\epsilon^3},$$

$$c_6 = \frac{7}{64\epsilon^5}, \quad c_8 = -\frac{5}{256\epsilon^7}, \quad c_3 = c_5 = c_7 = c_9 = 0.$$

The function $\phi(S) = \psi(S - K)$ smooths the payoff where asset price is at-the-money as shown in Fig. 1a.

For binary call option, define $\psi(x)$ as

$$\psi(x) = \begin{cases} Q & \text{for } x \geq \epsilon, \\ c_0 + c_1 x + c_2 x^2 + \ldots + c_9 x^9 & \text{for } -\epsilon < x < \epsilon, \\ 0 & \text{for } x \leq -\epsilon. \end{cases}$$

The following conditions will determine the function $\psi(x)$ uniquely:

$$\psi(-\epsilon) = \psi'(-\epsilon) = \psi''(-\epsilon) = \psi'''(-\epsilon) = \psi^{(4)}(-\epsilon) = 0$$

$$\psi(\epsilon) = Q, \psi'(\epsilon) = \psi''(\epsilon) = \psi'''(\epsilon) = \psi^{(4)}(\epsilon) = 0.$$

Solving these equations, we get

$$c_0 = \frac{Q}{2}, \quad c_1 = \frac{315Q}{256\epsilon}, \quad c_3 = \frac{-105Q}{64\epsilon^3}, \quad c_5 = \frac{189Q}{128\epsilon^5},$$

$$c_7 = \frac{-45Q}{64\epsilon^7}, \quad c_9 = \frac{35Q}{256\epsilon^9}, \quad c_2 = c_4 = c_6 = c_8 = 0.$$

The function $\phi(S) = \psi(S - K)$ smooths out the payoff of binary option at the point of jump discontinuity as shown in Fig. 1b.

The payoff diagram of butterfly option has singularity at three points $(S = K_1, K_2, K_3)$. Here we define the smoothing function as follows:

$$\phi(S) = \begin{cases} 0 & \text{for } S \leq K_1 - \epsilon, \\ \psi_1(S - K_1) & \text{for } K_1 - \epsilon < S < K_1 + \epsilon, \\ S - K_1 & \text{for } K_1 + \epsilon \leq S \leq K_2 - \epsilon, \\ \psi_2(S - K_2) & \text{for } K_2 - \epsilon < S < K_2 + \epsilon, \\ K_3 - S & \text{for } K_2 + \epsilon \leq S \leq K_3 - \epsilon, \\ \psi_3(S - K_3) & \text{for } K_3 - \epsilon < S < K_3 + \epsilon, \\ 0 & \text{for } S \geq K_3 + \epsilon, \end{cases}$$

where $\psi_1(S - K_1) = \sum_{i=0}^{9} c_i (S - K_1)$ and the coefficients $c_i, i = 0, 1, \ldots, 9$ are computed by solving the following ten conditions:

$$\psi_1(-\epsilon) = \psi_1'(-\epsilon) = \psi_1''(-\epsilon) = \psi_1'''(-\epsilon) = \psi_1^{(4)}(-\epsilon) = 0$$

$$\psi_1(\epsilon) = \epsilon, \psi_1'(\epsilon) = 1, \psi_1''(\epsilon) = \psi_1'''(\epsilon) = \psi_1^{(4)}(\epsilon) = 0;$$

$\psi_2(S - K_2) = \sum_{i=0}^{9} d_i (S - K_2)$ and the coefficients $d_i, i = 0, 1, \ldots, 9$ are computed by solving the following ten conditions:

$$\psi_2(-\epsilon) = K_2 - K_1 - \epsilon, \psi_2'(-\epsilon) = 1, \psi_2''(-\epsilon) = \psi_2'''(-\epsilon) = \psi_2^{(4)}(-\epsilon) = 0$$

$$\psi_2(\epsilon) = K_2 - K_1 - \epsilon, \psi_2'(\epsilon) = -1, \psi_2''(\epsilon) = \psi_2'''(\epsilon) = \psi_2^{(4)}(\epsilon) = 0$$

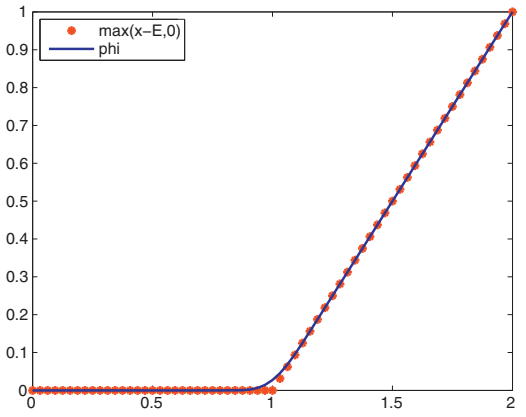

(a) smoothing the payoff of European option

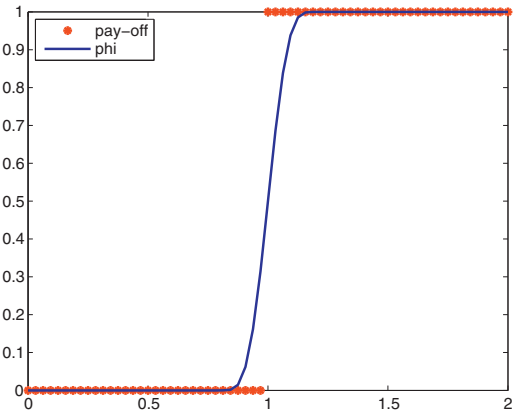

(b) smoothing the payoff of binary option

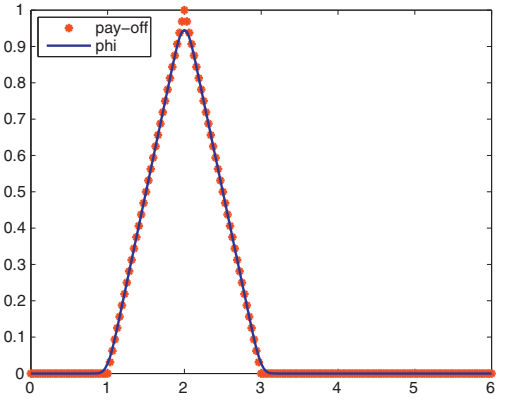

(c) smoothing the payoff of butterfly spread function

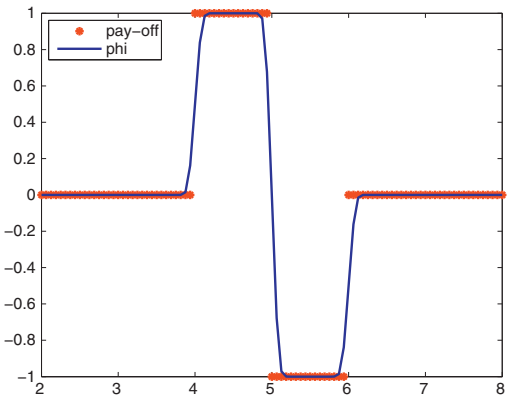

(d) smoothing the butterfly spread delta

Fig. 1. Payoff diagrams.

and $\psi_3(S-K_3)=\sum_{i=0}^{9}e_i(S-K_3)$ and the coefficients $e_i, i=0,1,\ldots,9$ are computed by solving the following ten conditions:

$$\psi_3(-\epsilon)=\epsilon,\ \psi_3'(-\epsilon)=-1,\ \psi_2''(-\epsilon)=\psi_2'''(-\epsilon)=\psi_2^{(4)}(-\epsilon)=0$$

$$\psi_3(\epsilon)=\psi_3'(\epsilon)=\psi_3''(\epsilon)=\psi_3'''(\epsilon)=\psi_3^{(4)}(\epsilon)=0.$$

The coefficients c_i, d_i and $e_i, i=0,1,\ldots,9$ take the following values:

$$c_0=\frac{35}{256}\epsilon,\quad c_1=\frac{1}{2},\quad c_2=\frac{35}{64\epsilon},\quad c_4=-\frac{35}{128\epsilon^3},$$

$$c_6=\frac{7}{64\epsilon^5},\quad c_8=-\frac{5}{256\epsilon^7},\quad c_3=c_5=c_7=c_9=0;$$

$$d_0=\frac{64(K_3-K_1)-35\epsilon}{128}\epsilon,\quad d_1=\frac{315(K_1-2K_2+K_3)}{256\epsilon},\quad d_2=\frac{-35}{32\epsilon},$$

$$d_3=\frac{-(105(K_1-2K_2+K_3))}{64\epsilon^3},\quad d_4=\frac{35}{64\epsilon^3},\quad d_5=\frac{189(K_1-2K_2+K_3)}{128\epsilon^5},$$

$$d_6 = \frac{-7}{32\epsilon^5}, \quad d_7 = \frac{-(45(K_1 - 2K_2 + K_3))}{64\epsilon^7}, \quad d_8 = \frac{5}{128\epsilon^7}, \quad d_9 = \frac{35(K_1 - 2K_2 + K_3)}{256\epsilon^9}$$

and

$$e_0 = \frac{35}{256}\epsilon, \quad e_1 = \frac{-1}{2}, \quad e_2 = \frac{35}{64\epsilon}, \quad e_4 = -\frac{35}{128\epsilon^3},$$

$$e_6 = \frac{7}{64\epsilon^5}, \quad e_8 = -\frac{5}{256\epsilon^7}, \quad e_3 = e_5 = e_7 = e_9 = 0.$$

Here the function $\phi(S)$ smooths out the butterfly spread payoff at all the three points of singularity as shown in Fig. 1c.

Similarly we create a function which smooths out the butterfly spread delta function defined above at the three points of singularity $S1$, $S2$ and $S3$, and is shown in Fig. 1d.

Now the problem (2.1) takes the form

$$\frac{1}{2}\sigma^2(S,\tau)S^2\frac{\partial^2\hat{C}}{\partial S^2} + (r(S,\tau) - D(S,\tau))S\frac{\partial\hat{C}}{\partial S} - r(S,\tau)\hat{C} = -\frac{\partial\hat{C}}{\partial\tau}, \quad S > 0, \tau \in (0,T) \tag{2.3a}$$

along with the final condition

$$\hat{C}(S,T) = \phi(S), \qquad S \in [0,\infty) \tag{2.3b}$$

and the corresponding boundary conditions of different option styles. The existence and uniqueness of classical solution of (2.3) was given in [30]. The error estimate due to this smoothing of the final condition in European option case is given by

$$|C(S,\tau) - \hat{C}(S,\tau)| \le \kappa\|\phi(S) - \max(S-K,0)\|_{L^\infty}, \qquad (S,\tau) \in [0,\infty) \times [0,T],$$

where κ is a positive constant independent of ϕ ([30,31]).

To apply numerical scheme, we need to truncate asset price domain $[0, \infty)$ to $[0, S_{max}]$, where S_{max} is chosen sufficiently large; also suitable boundary conditions are to be applied [32]. Thus the problem takes the form

$$\frac{1}{2}\sigma^2(S,\tau)S^2\frac{\partial^2 c}{\partial S^2} + (r(S,\tau) - D(S,\tau))S\frac{\partial c}{\partial S} - r(S,\tau)c = -\frac{\partial c}{\partial\tau}, \quad S \in (0,S_{max}), \tau \in [0,T) \tag{2.4a}$$

with the final condition

$$c(S,T) = \phi(S), \qquad S \in [0,S_{max}]; \tag{2.4b}$$

and the boundary conditions

$$c(0,\tau) = g_1(\tau), \qquad \tau \in [0,T] \tag{2.4c}$$

and

$$c(S_{max},\tau) = g_2(\tau), \qquad \tau \in [0,T]. \tag{2.4d}$$

Here $g_1(\tau) = 0$ for all the four cases of options we are referring but $g_2(\tau)$ has following different values for different options:

$$g_2(\tau) = S_{max}\exp\left(-\int_\tau^T D(S_{max},y)dy\right) - K\exp\left(-\int_\tau^T r(S_{max},y)dy\right), \ \tau \in [0,T]$$

for European option,

$$g_2(\tau) = Q\exp\left(-\int_\tau^T r(S_{max},q)dq\right), \ \tau \in [0,T] \ \text{ for binary option}$$

and

$$g_2(\tau) = 0, \ \tau \in [0,T]$$

for butterfly spread and portfolio of options with butterfly spread delta function as the final condition.

Let $(S,\tau) \in (0,S_{max}) \times [0,T]$ be any interior point satisfying

$$\ln\frac{S_{max}}{S} \ge -\zeta(T-\tau)$$

where

$$\zeta = \inf\{\sigma^2(S,\tau) - 2r(S,\tau) + 2D(S,\tau) : (S,\tau) \in (0,S_{max}) \times (0,T)\}.$$

Then the estimate for the error between the solutions of the problems (2.3) and (2.4) is given by ([33])

$$|\hat{C}(S,\tau)-c(S,\tau)| \le \|\hat{C}-c\|_{L^\infty(\{S_{max}\}\times(\tau,T))} \exp\left(-\frac{\ln\frac{S_{max}}{S}\left(\ln\frac{S_{max}}{S}+\min\{0,\zeta\}(T-\tau)\right)}{2\|\sigma^2\|_\infty(T-\tau)}\right).$$

Apply the transformation $\tau = T-t$, where t is the new time variable. Introduce the following new variables:

$$\begin{aligned}
&u(S,t) = c(S,\tau),\\
&\hat{\sigma}(S,t) = \sigma(S,\tau),\\
&\hat{r}(S,t) = r(S,\tau),\\
&\hat{D}(S,t) = D(S,\tau),\\
&\hat{g_1}(t) = g_1(\tau),\\
&\hat{g_2}(t) = g_2(\tau).
\end{aligned}$$

Then the above final boundary value problem is changed into initial boundary value problem given as follows:

$$\frac{1}{2}\hat{\sigma}^2(S,t)S^2\frac{\partial^2 u}{\partial S^2} + (\hat{r}(S,t)-\hat{D}(S,t))S\frac{\partial u}{\partial S} - \hat{r}(S,t)u = \frac{\partial u}{\partial t}, \qquad S\in(0,S_{max}), t\in(0,T), \tag{2.5a}$$

with the initial condition

$$u(S,0) = \phi(S), \qquad S\in[0,S_{max}]; \tag{2.5b}$$

and the boundary conditions

$$u(0,t) = \hat{g_1}(t), \qquad t\in[0,T] \tag{2.5c}$$

and

$$u(S_{max},t) = \hat{g_2}(t), \qquad t\in[0,T]. \tag{2.5d}$$

Here $\hat{g_1}=0$ for the four option styles we are discussing and $\hat{g_2}$ is defined as follows for different options:

$$\hat{g_2}(t) = S_{max}\exp\left(-\int_0^t \hat{D}(S_{max},q)dq\right) - K\exp\left(-\int_0^t \hat{r}(S_{max},q)dq\right),\ t\in[0,T] \tag{2.6}$$

for European option,

$$\hat{g_2}(t) = Q\exp\left(-\int_0^t \hat{r}(S_{max},q)dq\right),\ t\in[0,T] \text{ for binary option} \tag{2.7}$$

and

$$\hat{g_2}(t) = 0,\ t\in[0,T] \tag{2.8}$$

for butterfly spread and portfolio of options with butterfly spread delta function as the final condition. The existence and uniqueness of the analytical solution of truncated problem (2.5) was established in [27].

Define $\Omega = (0,S_{max})\times(0,T]$. Now the problem to be solved is

$$Lu(S,t) \equiv \frac{\partial u}{\partial t} - a_2(S,t)\frac{\partial^2 u}{\partial S^2} - a_1(S,t)\frac{\partial u}{\partial S} - a_0(S,t)u = f(S,t), \qquad (S,t)\in\Omega \tag{2.9a}$$

where

$$\begin{aligned}
&a_2(S,t) = \frac{1}{2}\hat{\sigma}^2S^2,\\
&a_1(S,t) = (\hat{r}-\hat{D})S,\\
&a_0(S,t) = -\hat{r},
\end{aligned}$$

with the initial condition

$$u(S,0) = \phi(S), \qquad S\in[0,S_{max}]; \tag{2.9b}$$

and the boundary conditions

$$u(0,t) = \hat{g_1}(t), \qquad t\in[0,T] \tag{2.9c}$$

and

$$u(S_{max},t) = \hat{g_2}(t), \qquad t\in[0,T], \tag{2.9d}$$

where $\hat{g_1}$ and $\hat{g_2}$ are as defined above.

Let us assume that $a_2(S,t)\ge 0, a_1(S,t)\ge 0$ and $-a_0(S,t) > 0$. Further assume that the problem (2.9) satisfy sufficient regularity conditions and the following compatibility conditions

$$\phi(0) = \hat{g_1}(0) \quad \text{and} \quad \phi(S_{max}) = \hat{g_2}(0) \tag{2.10}$$

which guarantee the problem has a unique solution $u\in C(\bar{\Omega})\cap C^{2,1}(\Omega)$ satisfying [27,30]

$$\left|\frac{\partial^{m+n}u}{\partial S^m\partial t^n}(S,t)\right| \le \mathscr{C} \text{ on } \bar{\Omega};\ 0\le n\le 3 \text{ and } 0\le m+n\le 4. \tag{2.11}$$

3. Discretization

Let the partition Ω_h in the space direction be $0 = S_0 < S_1 < ... < S_{m-1} < S_m < S_{m+1} < ... < S_M = S_{max}$, where M is the total number of intervals. This is a uniform discretization with constant grid spacing $h = \frac{S_{m+1}-S_m}{M}$ for all $m = 0, 1, \ldots, M-1$. Let the partition Ω^k in the time direction be $0 = t_0 < t_1 < ... < t_{n-1} < t_n < t_{n+1} < ... < t_N = T$, where N is total number of intervals. This is also uniform discretization with constant grid spacing $k = \frac{t_{n+1}-t_n}{N}$ for all $n = 0, 1, \ldots, N-1$. Denote the tensor product of Ω_h and Ω^k by Ω_h^k. The discrete approximation of option price $u(S, t)$ at the point (S_m, t_n) is written as $U(S_m, t_n)$.

Now onwards, we use the following notations:

$$
\begin{aligned}
&U(S_m, t_n) = U_m^n,\\
&u(S_m, t_n) = u_m^n,\\
&v(S_m, t_n) = v_m^n,\\
&w(S_m, t_n) = w_m^n,\\
&a_2(S_m, t_n) = a_{2,m}^n,\\
&a_1(S_m, t_n) = a_{1,m}^n,\\
&a_0(S_m, t_n) = a_{0,m}^n,\\
&\phi(S_m) = \phi_m,\\
&\hat{g_1}(t_n) = \hat{g_1}^n,\\
&\hat{g_2}(t_n) = \hat{g_2}^n.
\end{aligned}
$$

The fully discrete scheme on this mesh is given by

$$
\begin{aligned}
\beta_{m,1}^n(\delta_t U_m^n) + \beta_{m,2}^n(\delta_t U_{m+1}^n) + [\alpha_{m,-}^n U_{m-1}^n + \alpha_{m,c}^n U_m^n + \alpha_{m,+}^n U_{m+1}^n] =\\
\beta_{m,1}^n f_m^n + \beta_{m,2}^n f_{m+1}^n, \quad m = 1, 2, \ldots, M-1, \ n = 1, 2, \ldots, N,
\end{aligned} \tag{3.1a}
$$

where

$$\delta_t U_m^n = (U_m^n - U_m^{n-1})/k, \quad n = 1,$$

$$\delta_t U_m^n = \left(\frac{3}{2}U_m^n - 2U_m^{n-1} + \frac{1}{2}U_m^{n-2}\right)/k, \quad n = 2, 3, \ldots, N,$$

$$U_m^0 = \phi_m, \quad m = 0, 1, \ldots, M, \tag{3.1b}$$

$$U_0^n = \hat{g_1}^n, \quad n = 0, 1, \ldots, N, \tag{3.1c}$$

$$U_M^n = \hat{g_1}^n, \quad n = 0, 1, \ldots, N. \tag{3.1d}$$

Here, second time level onwards, the time direction is discretized using two-step backward differentiation formula. And backward Euler's formula is used for the solution at the first time level.

Space discretization is done using the classical HODIE (High-Order Difference approximation with Identity Expansion) scheme [24,25,34] with three stencil points (adjacent mesh points in the space direction) (S_{m-1}, t_n), (S_m, t_n) and (S_{m+1}, t_n) and two auxiliary points (points between first and last stencil point) (S_m, t_n) and (S_{m+1}, t_n), $m = 1, 2, \ldots, M-1$ at each time level t_n, $n = 1, 2, \ldots, N$.

The HODIE coefficients $\alpha_{m,-}^n$, $\alpha_{m,c}^n$ and $\alpha_{m,+}^n$ are the three coefficients of approximate solution U at the three stencil points at n^{th} time level. The HODIE coefficients $\beta_{m,1}^n$ and $\beta_{m,2}^n$ are the two coefficients for identity expansion at the two auxiliary points at n^{th} time level. These coefficients are computed for every $m = 1, 2, \ldots, M-1$ and at every time level $n = 1, 2, ..., N$. For simplicity, transform the space interval $[S_{m-1}, S_{m+1}]$ into $[-h, h]$ ([34]). The HODIE coefficients $\alpha's$ and $\beta's$, are computed "locally" by making (3.1a) exact on P_3, the space of polynomials (in the space variable) of degree less than or equal to 3, as shown below

$$\alpha_{m,-}^n + \alpha_{m,c}^n + \alpha_{m,+}^n = \beta_{m,1}^n(-a_{0,m}^n) + \beta_{m,2}^n(-a_{0,m+1}^n), \tag{3.2}$$

$$-h\alpha_{m,-}^n + h\alpha_{m,+}^n = \beta_{m,1}^n(-a_{1,m}^n) + \beta_{m,2}^n(-a_{1,m+1}^n - ha_{0,m+1}^n), \tag{3.3}$$

$$h^2\alpha_{m,-}^n + h^2\alpha_{m,+}^n = \beta_{m,1}^n(-2a_{2,m}^n) + \beta_{m,2}^n(-2a_{2,m+1}^n - 2ha_{1,m+1}^n - h^2a_{0,m+1}^n), \tag{3.4}$$

$$-h^3\alpha_{m,-}^n + h^3\alpha_{m,+}^n = \beta_{m,2}^n(-6ha_{2,m+1}^n - 3h^2a_{1,m+1}^n - h^3a_{0,m+1}^n) \tag{3.5}$$

for $m = 1, 2, \ldots, M-1$ and $n = 1, 2, \ldots, N$. In order to compute these coefficients $\alpha's$ and $\beta's$ uniquely we use the normalization condition

$$\beta^n_{m,1} + \beta^n_{m,2} = 1, \qquad m = 1, 2, \ldots, M-1, \ n = 1, 2, \ldots, N. \tag{3.6}$$

The above equations lead us to the following values:

$$\alpha^n_{m,-} = \frac{\beta^n_{m,1}(-2a^n_{2,m} + ha^n_{1,m}) + \beta^n_{m,2}(-2a^n_{2,m+1} - ha^n_{1,m+1})}{2h^2}, \tag{3.7}$$

$$\alpha^n_{m,+} = \frac{\beta^n_{m,1}(-2a^n_{2,m} - ha^n_{1,m}) + \beta^n_{m,2}(-2a^n_{2,m+1} - 3ha^n_{1,m+1} - 2h^2a^n_{0,m+1})}{2h^2}, \tag{3.8}$$

$$\alpha^n_{m,c} = \frac{\beta^n_{m,1}(4a^n_{2,m} - 2h^2a^n_{0,m}) + \beta^n_{m,2}(4a^n_{2,m+1} + 4ha^n_{1,m+1})}{2h^2}, \tag{3.9}$$

$$\beta^n_{m,1} = \frac{6ha^n_{2,m+1} + 2h^2a^n_{1,m+1}}{6ha^n_{2,m+1} + 2h^2a^n_{1,m+1} + h^2a^n_{1,m}} \tag{3.10}$$

and

$$\beta^n_{m,2} = \frac{h^2a^n_{1,m}}{6ha^n_{2,m+1} + 2h^2a^n_{1,m+1} + h^2a^n_{1,m}}. \tag{3.11}$$

With these HODIE coefficients, (3.1a) takes the form

$$L^k_hU^n_m \equiv \alpha^n_{m,-}U^n_{m-1} + \left(\alpha^n_{m,c} + \frac{1}{k}\beta^n_{m,1}\right)U^n_m + (\alpha^n_{m,+} + \frac{1}{k}\beta^n_{m,2})U^n_{m+1} =$$
$$\beta^n_{m,1}\left(f^n_m + \frac{1}{k}U^{n-1}_m\right) + \beta^n_{m,2}\left(f^n_{m+1} + \frac{1}{k}U^{n-1}_{m+1}\right) = F^n_m \text{ (say)}, \qquad m = 1, 2, \ldots, M-1, \ n = 1. \tag{3.12}$$

and

$$L^k_hU^n_m \equiv \alpha^n_{m,-}U^n_{m-1} + \left(\alpha^n_{m,c} + \frac{3}{2k}\beta^n_{m,1}\right)U^n_m + (\alpha^n_{m,+} + \frac{3}{2k}\beta^n_{m,2})U^n_{m+1} =$$
$$\beta^n_{m,1}\left(f^n_m + \frac{2}{k}U^{n-1}_m - \frac{1}{2k}U^{n-2}_m\right) + \beta^n_{m,2}\left(f^n_{m+1} + \frac{2}{k}U^{n-1}_{m+1} - \frac{1}{2k}U^{n-2}_{m+1}\right) =$$
$$F^n_m \text{ (say)}, \qquad m = 1, 2, \ldots, M-1, \ n = 2, 3, \ldots, N. \tag{3.13}$$

This is equivalent to solving a system of $M-1$ linear equations in $M-1$ unknowns U^n_m, $m = 1, 2, \ldots, M-1$, at each time level $n = 1, 2, \ldots, N$, given by

$$A^nU^n = b^n, \qquad n = 1, 2, \ldots, N, \tag{3.14}$$

where for $m = 1$ and $m = M-1$, the terms involving U^n_0 and U^n_M have been moved to the right hand side. A^n, the matrix associated with the discrete operator, is a square matrix of order $M-1$ at n^{th} time level, U^n is the $(M-1)\times 1$ vector of unknown approximate solution at n^{th} time level and b^n is the $(M-1)\times 1$ vector at n^{th} time level consisting of known data and solution values at known time levels.

4. Error analysis

Lemma 4.1. *Assume that*

$$h\beta^n_{m,1}a^n_{1,m} \le 2(\beta^n_{m,1}a^n_{2,m} + \beta^n_{m,2}a^n_{2,m+1}) + h\beta^n_{m,2}a^n_{1,m+1}, \ m = 1, 2, \ldots, M-1, \ n = 1, 2, \ldots, N, \tag{4.1}$$

and

$$\beta^n_{m,2}\left(-a^n_{0,m+1} + \frac{3}{2k}\right) \le \frac{2(\beta^n_{m,1}a^n_{2,m} + \beta^n_{m,2}a^n_{2,m+1}) + h(\beta^n_{m,1}a^n_{1,m} + 3\beta^n_{m,2}a^n_{1,m+1})}{2h^2},$$
$$m = 1, 2, \ldots, M-1, \ n = 2, 3, \ldots, N. \tag{4.2}$$

then

$$\alpha^n_{m,-} \le 0, \ m = 1, 2, \ldots, M-1, \ n = 1, 2, \ldots, N, \tag{4.3}$$

$$\alpha^n_{m,+} + \frac{3}{2k}\beta^n_{m,2} \le 0, \ m = 1, 2, \ldots, M-1, \ n = 2, 3, \ldots, N. \tag{4.4}$$

Proof. The inequalities (4.3) and (4.4) can be easily obtained from (3.7), (3.8), (4.1) and (4.2). □

Remark. Similarly assume that

$$\beta^n_{m,2}\left(-a^n_{0,m+1}+\frac{1}{k}\right) \le \frac{2(\beta^n_{m,1}a^n_{2,m}+\beta^n_{m,2}a^n_{2,m+1})+h(\beta^n_{m,1}a^n_{1,m}+3\beta^n_{m,2}a^n_{1,m+1})}{2h^2},$$
$$m=1,2,\ldots,M-1,\ \ n=1, \tag{4.5}$$

then

$$\alpha^n_{m,+}+\frac{1}{k}\beta^n_{m,2}\le 0,\ \ m=1,2,\ldots,M-1,\ \ n=1. \tag{4.6}$$

Lemma 4.2. *(Discrete Maximum Principle). Under the assumptions of the Lemma 4.1, the operator L^k_h defined by (3.12)–(3.13) satisfies discrete maximum principle, that is if v^n_m and w^n_m are mesh functions that satisfy $v^n_0\le w^n_0,\ v^n_M\le w^n_M\ (n=0,1,...,N),\ v^0_m\le w^0_m,\ (m=0,1,\ldots,M)$ and $L^k_h v^n_m\le L^k_h w^n_m\ (m=1,2,\ldots,M-1,\ n=1,2,\ldots,N)$, then $v^n_m\le w^n_m$ for all m, n.*

Proof. The equations $L^k_h v^n_m=F^n_m,\ m=1,2,\ldots,M-1$, or more precisely, $A^n v^n=b^n$ is a system of $M-1$ linear equations in $M-1$ unknowns v^n_m for all $n=1,2,\ldots,N$, given by (3.12)–(3.13) and (3.14). Now we have tridiagonal coefficient matrices $A^n,\ n=1,2,\ldots,N$, where for $n=2,3,\ldots,N$,

$$A^n=\begin{bmatrix} \alpha^n_{1,c}+\frac{3}{2k}\beta^n_{1,1} & \alpha^n_{1,+}+\frac{3}{2k}\beta^n_{1,2} & 0 & \cdots & 0\\ \alpha^n_{2,-} & \alpha^n_{2,c}+\frac{3}{2k}\beta^n_{2,1} & \alpha^n_{2,+}+\frac{3}{2k}\beta^n_{2,2} & & \vdots\\ 0 & \ddots & \ddots & \ddots & 0\\ \vdots & & \alpha^n_{M-2,-} & \alpha^n_{M-2,c}+\frac{3}{2k}\beta^n_{M-2,1} & \alpha^n_{M-2,+}+\frac{3}{2k}\beta^n_{M-2,2}\\ 0 & \cdots & 0 & \alpha^n_{M-1,-} & \alpha^n_{M-1,c}+\frac{3}{2k}\beta^n_{M-1,1} \end{bmatrix}$$

and for $n=1$,

$$A^n=\begin{bmatrix} \alpha^n_{1,c}+\frac{1}{k}\beta^n_{1,1} & \alpha^n_{1,+}+\frac{1}{k}\beta^n_{1,2} & 0 & \cdots & 0\\ \alpha^n_{2,-} & \alpha^n_{2,c}+\frac{1}{k}\beta^n_{2,1} & \alpha^n_{2,+}+\frac{1}{k}\beta^n_{2,2} & & \vdots\\ 0 & \ddots & \ddots & \ddots & 0\\ \vdots & & \alpha^n_{M-2,-} & \alpha^n_{M-2,c}+\frac{1}{k}\beta^n_{M-2,1} & \alpha^n_{M-2,+}+\frac{1}{k}\beta^n_{M-2,2}\\ 0 & \cdots & 0 & \alpha^n_{M-1,-} & \alpha^n_{M-1,c}+\frac{1}{k}\beta^n_{M-1,1} \end{bmatrix}$$

The row sum of $A^n,\ n=2,3,\ldots,N$ is given by

$$\alpha^n_{m,-}+\alpha^n_{m,c}+\frac{3}{2k}\beta^n_{m,1}+\alpha^n_{m,+}+\frac{3}{2k}\beta^n_{m,2}>0,\quad m=1,2,...,M-1 \tag{4.7}$$

and the row sum of A^1 is given by

$$\alpha^1_{m,-}+\alpha^1_{m,c}+\frac{1}{k}\beta^1_{m,1}+\alpha^1_{m,+}+\frac{1}{k}\beta^1_{m,2}>0,\quad m=1,2,...,M-1. \tag{4.8}$$

Now (4.3), (4.4), (4.6), (4.7) and (4.8) conclude that the matrix $A^n,\ n=1,2,\ldots,N$ is diagonally dominant and has non positive off diagonal entries. Therefore, the matrix $A^n,\ n=1,2,\ldots,N$ is an irreducible M-matrix ([35,36]), consequently it has a positive inverse. Hence the solution $U^n_m,\ m=1,2,\ldots,M-1$ of (3.12) and (3.13) exist for each $n=1,2,\ldots,N$ and if the v^n_m and the w^n_m are as described in the lemma then $v^n_m\le w^n_m$ for all m, n. □

Lemma 4.3. *Let $v(S,t)$ be a sufficiently smooth function defined on Ω^k_h. Then the following estimate for the global truncation error holds true:*

$$\begin{aligned}|L^k_h v^n_m-(Lv)^n_m| \le{}& \mathscr{C}_1 k^2\int_0^1\left[\left|\frac{\partial^3 v}{\partial t^3}(S_m,t_n-kx)\right|+\left|\frac{\partial^3 v}{\partial t^3}(S_m,t_n-2kx)\right|\right.\\ &\left.+\left|\frac{\partial^3 v}{\partial t^3}(S_m+hx,t_n-kx)\right|+\left|\frac{\partial^3 v}{\partial t^3}(S_m+hx,t_n-2kx)\right|\right]dx\\ &+\mathscr{C}_2 h^2\int_0^1\left[\left|\frac{\partial^3 v}{\partial S^2\partial t}(S_m+hx,t_n-kx)\right|+\left|\frac{\partial^3 v}{\partial S^2\partial t}(S_m+hx,t_n-2kx)\right|\right.\\ &\left.+\left|\frac{\partial^3 v}{\partial S^2\partial t}(S_m+hx,t_n)\right|+S^2_{m+1}\left|\frac{\partial^4 v}{\partial S^4}(S_m+hx,t_n)\right|\right]dx,\\ &m=1,2,\ldots,M-1,\ \ n=2,3,\ldots,N,\end{aligned} \tag{4.9}$$

where $\mathscr{C}_1$, and $\mathscr{C}_2$ are positive constants independent of the mesh parameters h and k.

Proof. The proof follows using Taylor's theorem in several variables with integral form of remainder. □

Theorem 4.4. *Let u be the solution of the continuous problem (2.9) and U_m^n be the solution of the discrete problem (3.1). Then under the assumptions (2.11),*

$$|u_m^n - U_m^n| \le \mathscr{C}(k^2 + h^2), \quad m = 0, 1, \ldots, M, \ \ n = 0, 1, \ldots, N, \tag{4.10}$$

where $\mathscr{C}$ is a positive constant independent of k and h.

Proof. Using (2.11) and the Lemma 4.3, we have

$$\begin{aligned}
\left|L_h^k(u_m^n - U_m^n)\right| &= \left|L_h^k u_m^n - (Lu)_m^n\right| \\
&\le \mathscr{C}_1 k^2 \int_0^1 \left[\left|\frac{\partial^3 u}{\partial t^3}(S_m, t_n - kx)\right| + \left|\frac{\partial^3 u}{\partial t^3}(S_m, t_n - 2kx)\right|\right. \\
&\quad \left. + \left|\frac{\partial^3 u}{\partial t^3}(S_m + hx, t_n - kx)\right| + \left|\frac{\partial^3 u}{\partial t^3}(S_m + hx, t_n - 2kx)\right|\right] dx \\
&\quad + \mathscr{C}_2 h^2 \int_0^1 \left[\left|\frac{\partial^3 u}{\partial S^2 \partial t}(S_m + hx, t_n - kx)\right| + \left|\frac{\partial^3 u}{\partial S^2 \partial t}(S_m + hx, t_n - 2kx)\right|\right. \\
&\quad \left. + \left|\frac{\partial^3 u}{\partial S^2 \partial t}(S_m + hx, t_n)\right| + S_{m+1}^2 \left|\frac{\partial^4 u}{\partial S^4}(S_m + hx, t_n)\right|\right] dx \\
&\le \mathscr{C}_3(k^2 + h^2) \qquad m = 1, 2, \ldots, M-1, \ \ n = 2, 3, \ldots, N.
\end{aligned} \tag{4.11}$$

We have used the backward Euler method for evaluating the solution at $n = 1$. The backward Euler method has a one-step error of order two ([37]) and we apply it only at the first level.

Hence from (4.11), it follows that:

$$\left|L_h^k(u_m^n - U_m^n)\right| \le \mathscr{C}_4(k^2 + h^2) \qquad m = 1, 2, \ldots, M-1, \ \ n = 0, 1, \ldots, N. \tag{4.12}$$

Now using Lemma 4.2 over the barrier function

$$\mathscr{C}(h^2 + k^2)(1 + t_n) \pm (u_m^n - U_m^n),$$

we have

$$|u_m^n - U_m^n| \le \mathscr{C}(k^2 + h^2) \text{ for every } m = 1, 2, \ldots, M-1, \ \ n = 1, 2, \ldots, N. \tag{4.13}$$

□

5. Numerical experiments and discussion

First we illustrate two examples on Black–Scholes model. These examples are the particular case, where we know the closed form solution as given by (1.4). Setting $\tau = T - t$, the closed form solution (1.4), takes the form

$$u(S, t) = S\exp(-\hat{D}t)N(\hat{d_1}) - K\exp(-\hat{r}t)N(\hat{d_2}) \tag{5.1}$$

where

$$\hat{d_1} = \frac{\ln S - \ln K + \left(\hat{r} - \hat{D} + \frac{1}{2}\hat{\sigma}^2\right)t}{\hat{\sigma}\sqrt{t}}, \tag{5.2}$$

$$\hat{d_2} = \hat{d_1} - \hat{\sigma}\sqrt{t}. \tag{5.3}$$

Here

$$\hat{d_1}(S, t) = d_1(S, \tau), \quad \hat{d_2}(S, t) = d_2(S, \tau)$$

and $N(y)$ is as defined in Section 1. Here we compute the true maximum absolute error ($\hat{E}_{\max}^{M,N}$), root mean square error ($\hat{E}_{\text{rms}}^{M,N}$) and corresponding orders of convergence $\hat{p}_{\max}^{M,N}$ and $\hat{p}_{\text{rms}}^{M,N}$ as follows:

$$\hat{E}_{\max}^{M,N} = \max_{0 \le m \le M} \left|u^{M,N}(S_m, t_N) - U^{M,N}(S_m, t_N)\right|,$$

$$\hat{E}_{\text{rms}}^{M,N} = \sqrt{\frac{\sum_{m=0}^{M}\left[\left(u^{M,N}(S_m, t_N) - U^{M,N}(S_m, t_N)\right)^2\right]}{M+1}},$$

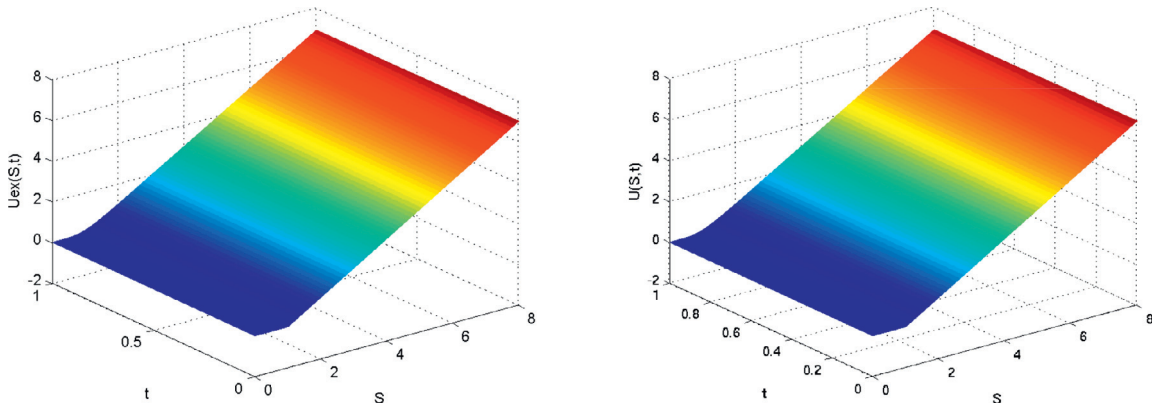

(a) Analytical solution of Example 5.1(a) (b) Numerical solution of Example 5.1(a)

Fig. 5.2. Analytical and Numerical solutions of Example 5.1(a).

Table 5.1
Maximum absolute errors ($\hat{E}_{\max}$, $E_{\max}$), root mean square errors ($\hat{E}_{\text{rms}}$, E_{rms}) and corresponding orders of convergence $\hat{p}_{\max}$, $p_{\max}$, $\hat{p}_{\text{rms}}$ and p_{rms} for Example 5.1(a).

M	2^4	2^5	2^6	2^7	2^8	2^9	2^{10}
N	10	10×2	10×2^2	10×2^3	10×2^4	10×2^5	10×2^6
$\hat{E}_{\max}$	3.4226e−02	7.4769e−03	1.7759e−03	4.4895e−04	1.1219e−04	2.8068e−05	7.0223e−06
$\hat{p}_{\max}$		2.1946	2.0739	1.9839	2.0006	1.9989	1.9989
$E_{\max}$		2.6749e−02	5.7118e−03	1.3347e−03	3.3676e−04	8.4126e−05	2.1048e−05
$p_{\max}$			2.2274	2.0973	1.9868	2.0011	1.9989
$\hat{E}_{\text{rms}}$	8.4476e-03	1.8556e−03	4.5900e−04	1.1499e−04	2.8825e−05	7.2183e−06	1.8061e−06
$\hat{p}_{\text{rms}}$		2.1867	2.0153	1.9970	1.9962	1.9975	1.9987
E_{rms}		6.5709e−03	1.4002e−03	3.4446e−04	8.6225e−05	2.1613e−05	5.4130e−06
p_{rms}			2.2304	2.0232	1.9982	1.9962	1.9974

$$\hat{p}^{M,N}_{\max}=\log_2\left(\frac{\hat{E}^{M,N}_{\max}}{\hat{E}^{2M,2N}_{\max}}\right)\ \text{and}\ \hat{p}^{M,N}_{\text{rms}}=\log_2\left(\frac{\hat{E}^{M,N}_{\text{rms}}}{\hat{E}^{2M,2N}_{\text{rms}}}\right).$$

Then, we give some more examples on pricing of different option styles discussed in Section 2 that follow the generalized Black–Scholes equation, where σ, r and D are functions of S and t. The analytical solution of the generalized Black–Scholes equation is not known, hence we use the double mesh principle to obtain the maximum absolute error ($E^{M,N}_{max}$), the root mean square error ($E^{M,N}_{rms}$), the order of convergence corresponding to maximum absolute error ($p^{M,N}_{max}$) and the order of convergence corresponding to root mean square error ($p^{M,N}_{rms}$).

$$E^{M,N}_{\max}=\max_{0\le m\le M}\left|U^{M,N}(S_m,t_N)-U^{2M,2N}(S_{2m},t_{2N})\right|,$$

$$E^{M,N}_{\text{rms}}=\sqrt{\frac{\sum_{m=0}^{M}\left[\left(U^{M,N}(S_m,t_N)-U^{2M,2N}(S_{2m},t_{2N})\right)^2\right]}{M+1}},$$

$$p^{M,N}_{\max}=\log_2\left(\frac{E^{M,N}_{\max}}{E^{2M,2N}_{\max}}\right)\ \text{and}\ p^{M,N}_{\text{rms}}=\log_2\left(\frac{E^{M,N}_{\text{rms}}}{E^{2M,2N}_{\text{rms}}}\right).$$

Example 5.1(a). Consider the Black–Scholes equation for European call option price (2.9) with $\hat{\sigma}(S,t)=0.4$, $\hat{r}(S,t)=0.04$, $\hat{D}(S,t)=0.02$, $T=1$ and $K=1$. Take $S_{max}=8$ and $\epsilon=10^{-6}$. The analytical solution and the numerical solution obtained using the scheme (3.1) are depicted in Fig. 5.2(a) and Fig. 5.2(b), respectively. The errors and the corresponding orders of convergence are displayed in Table 5.1.

Example 5.1(b). Consider the Black–Scholes equation for European call option price (2.9) with $\hat{\sigma}(S,t)=0.4$, $\hat{r}(S,t)=0.02$, $\hat{D}(S,t)=0.04$, $T=1$ and $K=1$. Take $S_{max}=8$ and $\epsilon=10^{-6}$. The analytical solution and the numerical solution obtained

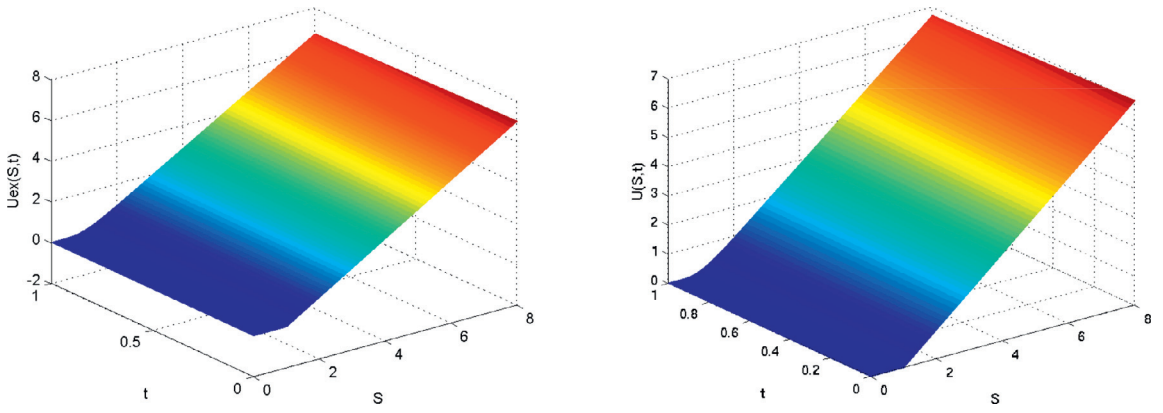

(a) Analytical solution of Example 5.1(b) (b) Numerical solution of Example 5.1(b)

Fig. 5.3. Analytical and Numerical solutions of Example 5.1(b).

Table 5.2
Maximum absolute errors ($\hat{E}_{\max}$, $E_{\max}$), root mean square errors ($\hat{E}_{\text{rms}}$, E_{rms}) and corresponding orders of convergence $\hat{p}_{\max}$, $p_{\max}$, $\hat{p}_{\text{rms}}$ and p_{rms} for Example 5.1(b).

M	2^4	2^5	2^6	2^7	2^8	2^9	2^{10}
N	10	10×2	10×2^2	10×2^3	10×2^4	10×2^5	10×2^6
$\hat{E}_{\max}$	3.7179e−02	8.0254e−03	1.8544e−03	4.5531e−04	1.1368e−04	2.8358e−05	7.0828e−06
$\hat{p}_{\max}$		2.2118	2.1136	2.0260	2.0018	2.0032	2.0014
$E_{\max}$		2.9153e−02	6.1709e−03	1.3991e−03	3.4214e−04	8.5325e−05	2.1276e−05
$p_{\max}$			2.2400	2.1409	2.0318	2.0035	2.0037
$\hat{E}_{\text{rms}}$	9.2068e−03	1.9795e−03	4.8207e−04	1.1978e−04	2.9896e−05	7.4703e−06	1.8672e−06
$\hat{p}_{\text{rms}}$		2.2176	2.0378	2.0089	2.0024	2.0007	2.0003
E_{rms}		7.1735e−03	1.5014e−03	3.6277e−04	8.9941e−05	2.2433e−05	5.6041e−06
p_{rms}			2.2563	2.0492	2.0119	2.0033	2.0010

Table 5.3
Maximum absolute error ($E_{\max}$), root mean square error (E_{rms}) and corresponding orders of convergence $p_{\max}$ and p_{rms} for Example 5.2(a).

M	2^3	2^4	2^5	2^6	2^7	2^8	2^9
N	5	5×2	5×2^2	5×2^3	5×2^4	5×2^5	5×2^6
$E_{\max}$		3.5462e−02	9.5302e−03	1.7006e−03	4.3432e−04	1.1027e−04	2.7757e−05
$p_{\max}$			1.8957	2.4864	1.9693	1.9777	1.9901
E_{rms}		1.4056e−02	3.0348e−03	6.4511e−04	1.6476e−04	4.1422e−05	1.0408e−05
p_{rms}			2.2115	2.2340	1.9691	1.9919	1.9927

using the scheme (3.1) are depicted in Fig. 5.3(a) and Fig. 5.3(b), respectively. The errors and the corresponding orders of convergence are displayed in Table 5.2.

Observe that in Example 5.1(a), $\hat{r} > \hat{D}$ but in Example 5.1(b), $\hat{r} < \hat{D}$. Vázquez ([32]) suggested that, from financial point of view, it is correct to assume $r > D > 0$, which justifies our assumption $a_1 \geq 0$ (observe that $\hat{r} = r$ and $\hat{D} = D$ in these cases). But while performing these numerical experiments, we observe that this assumption is not necessary.

Example 5.2(a). Consider the generalized Black–Scholes equation for European call option price (2.9) with $\hat{\sigma}(S,t) = 0.4(2 + (T-t)\sin(S))$, $\hat{r}(S,t) = 0.06(1 + t\exp(-S))$, $\hat{D}(S,t) = 0.02\exp(-t-S)$, $T = 1$ and $K = 1$. Take $S_{max} = 8$ and $\epsilon = 10^{-6}$. The numerical solution obtained using the scheme (3.1) is depicted in Fig. 5.4. The errors and the corresponding orders of convergence are displayed in Table 5.3.

Example 5.2(b). Consider the generalized Black–Scholes equation for European call option price (2.9) with $\hat{\sigma}(S,t) = 0.6(\sin(2t) + \exp(-S))$, $\hat{r}(S,t) = 0.01(0.02 + \sin(10t)\exp(-S))$, $\hat{D}(S,t) = 0.01t\exp(-S)$, $T = 1$ and $K = 1$. Take $S_{max} = 8$ and $\epsilon = 10^{-6}$. The numerical solution obtained using the scheme (3.1) is depicted in Fig. 5.5. The errors and the corresponding orders of convergence are displayed in Table 5.4.

Example 5.3(a). Consider the generalized Black–Scholes equation for binary call option price (2.9) with $\hat{\sigma}(S,t) = 0.4(2 + (T-t)\sin(S))$, $\hat{r}(S,t) = 0.06(1 + t\exp(-S))$, $\hat{D}(S,t) = 0.02\exp(-t-S)$, $T = 1$, $K = 1$ and $Q = 1$. Take $S_{max} = 8$ and $\epsilon = 10^{-6}$.

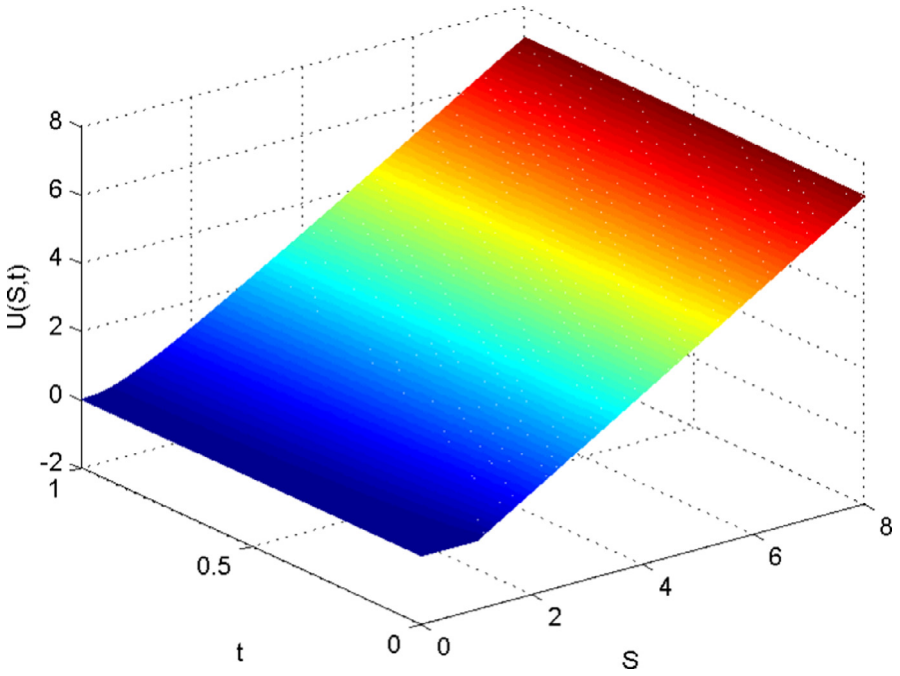

Fig. 5.4. Numerical solution of Example 5.2(a).

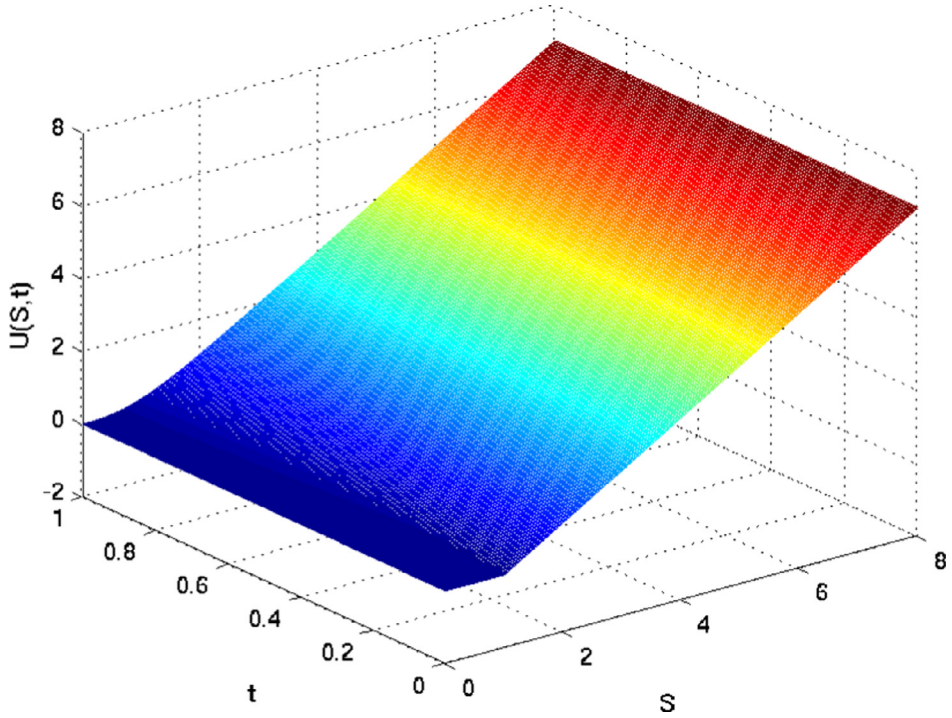

Fig. 5.5. Numerical solution of Example 5.2(b).

The numerical solution obtained using the scheme (3.1) is depicted in Fig. 5.6. The errors and the corresponding orders of convergence are displayed in Table 5.5.

Example 5.3(b). Consider the generalized Black–Scholes equation for binary call option price (2.9) with $\hat{\sigma}(S,t) = 0.6(\sin(2t) + \exp(-S))$, $\hat{r}(S,t) = 0.01(0.02 + \sin(10t)\exp(-S))$, $\hat{D}(S,t) = 0.01t\exp(-S)$, $T = 1$, $K = 1$ and $Q = 1$. Take $S_{max} =$

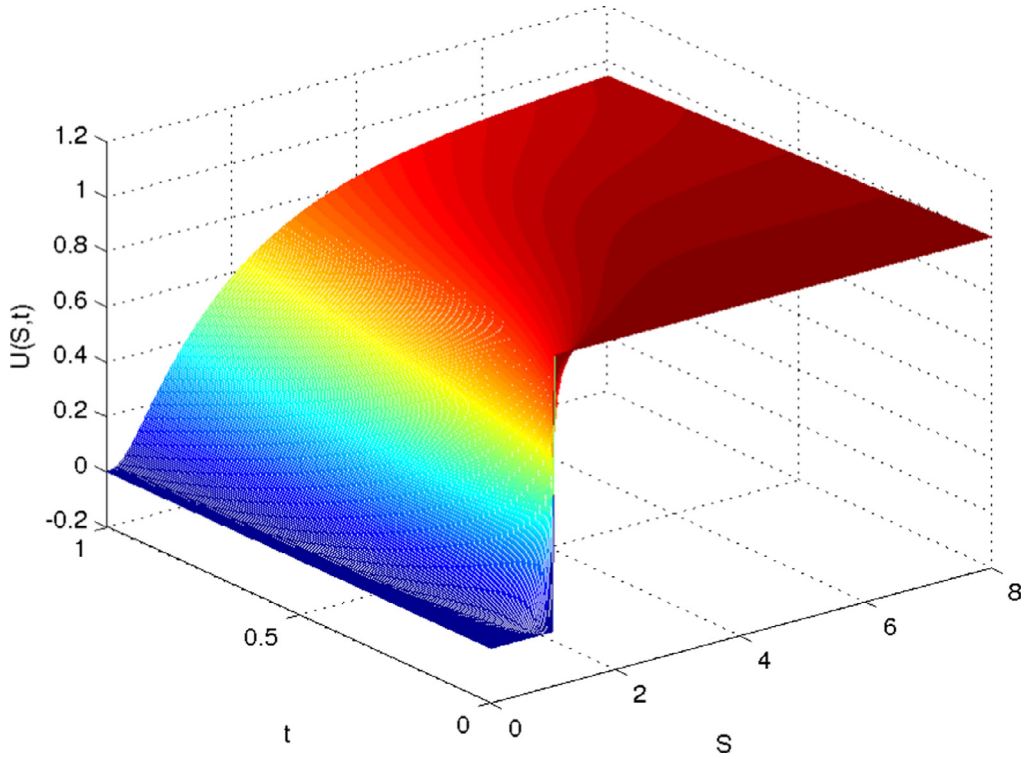

Fig. 5.6. Numerical solution of Example 5.3(a).

Table 5.4
Maximum absolute error ($E_{\max}$), root mean square error (E_{rms}) and corresponding orders of convergence $p_{\max}$ and p_{rms} for Example 5.2(b).

M	2^3	2^4	2^5	2^6	2^7	2^8	2^9
N	5	5×2	5×2^2	5×2^3	5×2^4	5×2^5	5×2^6
$E_{\max}$		5.7872e−02	1.4359e−02	3.1410e−03	7.7868e−04	1.9419e−04	4.8561e−05
$p_{\max}$			2.0109	2.1926	2.0121	2.0035	1.9996
E_{rms}		1.9366e−02	4.3084e−03	1.0625e−03	2.6598e−04	6.6712e−05	1.6716e−05
p_{rms}			2.1683	2.0197	1.9980	1.9953	1.9967

Table 5.5
Maximum absolute error ($E_{\max}$), root mean square error (E_{rms}) and corresponding orders of convergence $p_{\max}$ and p_{rms} for Example 5.3(a).

M	2^3	2^4	2^5	2^6	2^7	2^8	2^9
N	5	5×2	5×2^2	5×2^3	5×2^4	5×2^5	5×2^6
$E_{\max}$		9.2648e−02	1.5055e−02	4.1006e−03	1.0175e−03	2.5519e−04	6.3887e−05
$p_{\max}$			2.6215	1.8764	2.0108	1.9954	1.9980
E_{rms}		3.3401e−02	6.8631e−03	1.8592e−03	4.6289e−04	1.1663e−04	2.9269e−05
p_{rms}			2.2830	1.8842	2.0060	1.9887	1.9945

8 and $\epsilon = 10^{-6}$. The numerical solution obtained using the scheme (3.1) is depicted in Fig. 5.7. The errors and the corresponding orders of convergence are displayed in Table 5.6.

Example 5.4(a). Consider the generalized Black–Scholes equation for butterfly spread option price (2.9) with $\hat{\sigma}(S,t) = 0.4(2+(T-t)\sin(S))$, $\hat{r}(S,t) = 0.06(1+t\exp(-S))$, $\hat{D}(S,t) = 0.02\exp(-t-S)$, $T=1$, $K_1=1$, $K_2=2$ and $K_3=3$. Take $S_{max} = 8$ and $\epsilon = 10^{-6}$. The numerical solution obtained using the scheme (3.1) is depicted in Fig. 5.8. The errors and the corresponding orders of convergence are displayed in Table 5.7.

Example 5.4(b). Consider the generalized Black–Scholes equation for butterfly spread option price (2.9) with $\hat{\sigma}(S,t) = 0.6(\sin(2t)+\exp(-S))$, $\hat{r}(S,t) = 0.01(0.02+\sin(10t)\exp(-S))$, $\hat{D}(S,t) = 0.01t\exp(-S)$, $T=1$, $K_1=1$, $K_2=2$ and $K_3=3$. Take $S_{max} = 8$ and $\epsilon = 10^{-6}$. The numerical solution obtained using the scheme (3.1) is depicted in Fig. 5.9. The errors and the corresponding orders of convergence are displayed in Table 5.8.

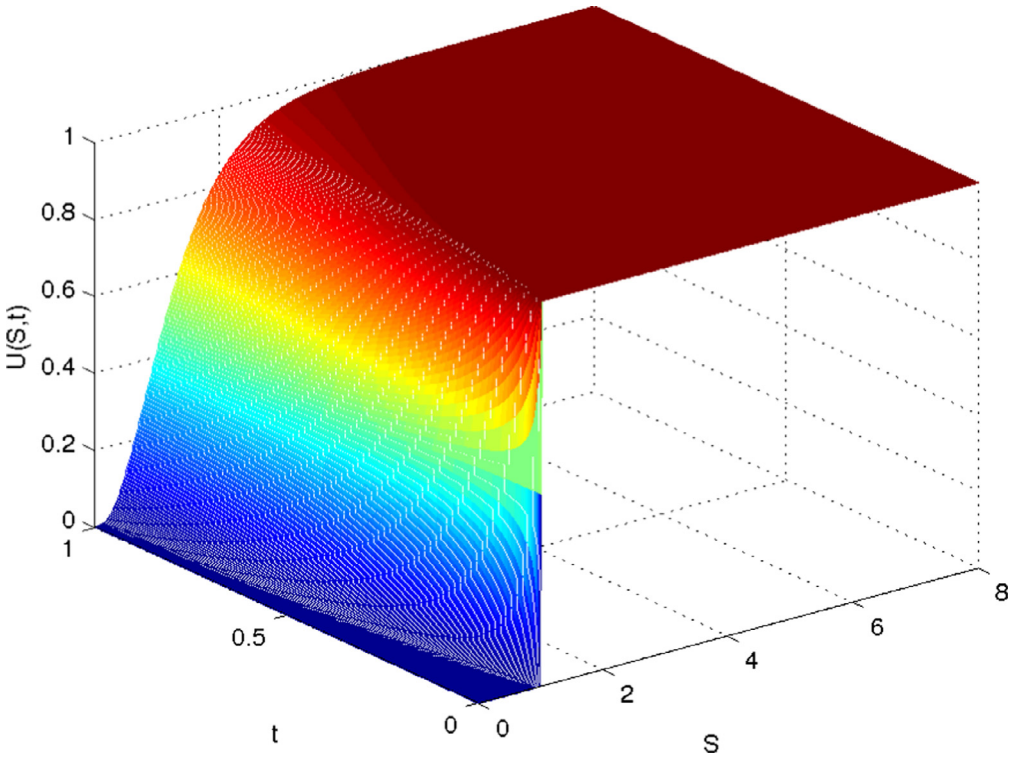

Fig. 5.7. Numerical solution of Example 5.3(b).

Table 5.6
Maximum absolute error (E_{max}), root mean square error (E_{rms}) and corresponding orders of convergence p_{max} and p_{rms} for Example 5.3(b).

M	2^3	2^4	2^5	2^6	2^7	2^8	2^9
N	5	5×2	5×2^2	5×2^3	5×2^4	5×2^5	5×2^6
E_{max}		4.4957e−02	1.8127e−02	3.4856e−03	8.5295e−04	2.1287e−04	5.3221e−05
p_{max}			1.3104	2.3786	2.0308	2.0025	1.9999
E_{rms}		1.7346e−02	5.4157e−03	1.1797e−03	2.9138e−04	7.2711e−05	1.8183e−05
p_{rms}			1.6794	2.1987	2.0174	2.0026	1.9995

Table 5.7
Maximum absolute error (E_{max}), root mean square error (E_{rms}) and corresponding orders of convergence p_{max} and p_{rms} for Example 5.4(a).

M	2^3	2^4	2^5	2^6	2^7	2^8	2^9
N	5	5×2	5×2^2	5×2^3	5×2^4	5×2^5	5×2^6
E_{max}		9.9529e−03	4.4412e−03	8.4272e−04	2.1721e−04	5.3340e−05	1.3578e−05
p_{max}			1.1641	2.3978	1.9559	2.0258	1.9739
E_{rms}		3.9974e−03	1.1239e−03	1.8367e−04	4.5319e−05	1.1674e−05	2.9728e−06
p_{rms}			1.8304	2.6133	2.0189	1.9568	1.9734

Table 5.8
Maximum absolute error (E_{max}), root mean square error (E_{rms}) and corresponding orders of convergence p_{max} and p_{rms} for Example 5.4(b).

M	2^3	2^4	2^5	2^6	2^7	2^8	2^9
N	5	5×2	5×2^2	5×2^3	5×2^4	5×2^5	5×2^6
E_{max}		6.7274e−02	9.6001e−03	2.4514e−03	5.9938e−04	1.4795e−04	3.6975e−05
p_{max}			2.8089	1.9694	2.0321	2.0184	2.0004
E_{rms}		2.8299e−02	4.5578e−03	1.0685e−03	2.6256e−04	6.5409e−05	1.6346e−05
p_{rms}			2.6343	2.0927	2.0248	2.0051	2.0005

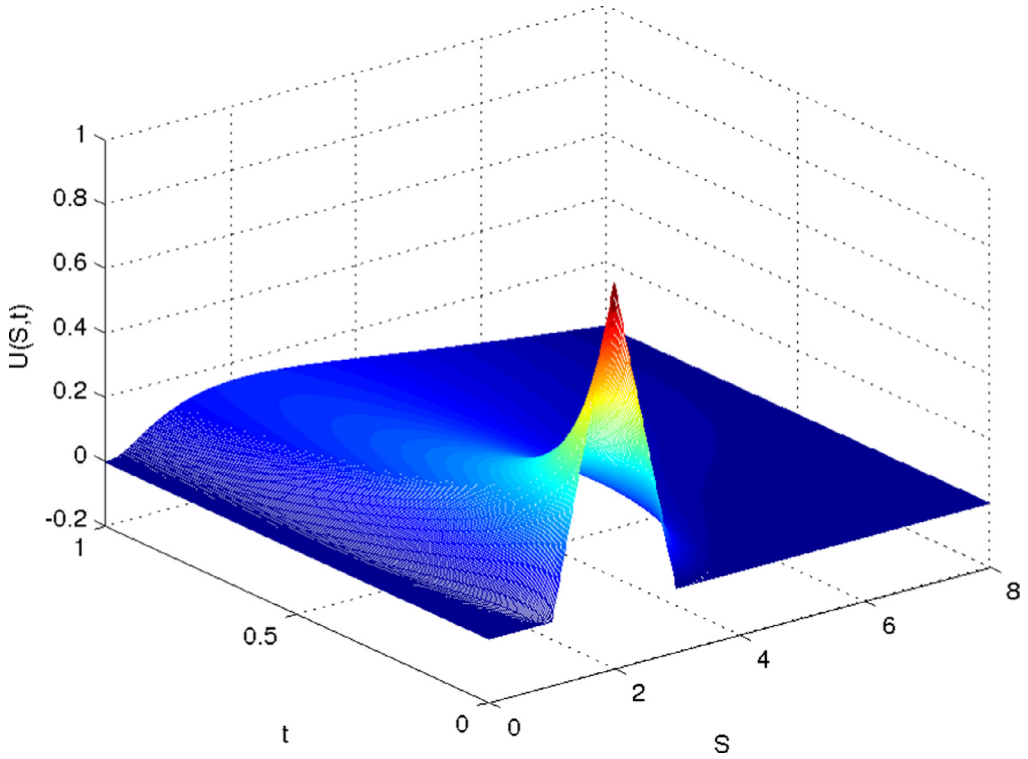

Fig. 5.8. Numerical solution of Example 5.4(a).

Table 5.9
Maximum absolute error ($E_{\max}$), root mean square error (E_{rms}) and corresponding orders of convergence $p_{\max}$ and p_{rms} for Example 5.5(a).

M	10	10×2	10×2^2	10×2^3	10×2^4	10×2^5	10×2^6
N	5	5×2	5×2^2	5×2^3	5×2^4	5×2^5	5×2^6
$E_{\max}$		2.3746e−02	6.6353e−03	1.8338e−03	4.8310e−04	1.2306e−04	3.0866e−05
$p_{\max}$			1.8395	1.8553	1.9244	1.9729	1.9953
E_{rms}		1.3511e−02	4.0740e−03	1.1679e−03	3.1117e−04	7.9619e−05	2.0004e−05
p_{rms}			1.7296	1.8026	1.9081	1.9665	1.9928

Table 5.10
Maximum absolute error ($E_{\max}$), root mean square error (E_{rms}) and corresponding orders of convergence $p_{\max}$ and p_{rms} for Example 5.5(b).

M	10	10×2	10×2^2	10×2^3	10×2^4	10×2^5	10×2^6
N	5	5×2	5×2^2	5×2^3	5×2^4	5×2^5	5×2^6
$E_{\max}$		6.8419e-03	1.6110e−03	2.8415e−04	6.7525e−05	1.6464e−05	4.0728e−06
$p_{\max}$			2.0864	2.5032	2.0732	2.0361	2.0152
E_{rms}		3.4224e−03	7.9965e−04	1.2504e−04	2.7488e−05	6.6294e−06	16360e−06
p_{rms}			2.0976	2.6770	2.1855	2.0518	2.0187

Example 5.5(a). Consider the generalized Black–Scholes equation (2.9) for portfolio of options with butterfly spread delta function as the final condition with $\hat{\sigma}(S,t) = 0.4(2+(T-t)\sin(S))$, $\hat{r}(S,t) = 0.06(1+t\exp(-S))$, $\hat{D}(S,t) = 0.02\exp(-t-S)$, $T=1$, $K=5$, $S1=4$, $S2=5$ and $S3=6$. Take $S_{max}=10$ and $\epsilon = 10^{-6}$. The numerical solution obtained using the scheme (3.1) is depicted in Fig. 5.10. The errors and the corresponding orders of convergence are displayed in Table 5.9.

Example 5.5(b). Consider the generalized Black–Scholes Eq. (2.9) for portfolio of options with butterfly spread delta function as the final condition with $\hat{\sigma}(S,t) = 0.6(\sin(2t)+\exp(-S))$, $\hat{r}(S,t) = 0.01(0.02+\sin(10t)\exp(-S))$, $\hat{D}(S,t) = 0.01t\exp(-S)$, $T=1$, $K=5$, $S1=4$, $S2=5$ and $S3=6$. Take $S_{max}=10$ and $\epsilon = 10^{-6}$. The numerical solution obtained using the scheme (3.1) is depicted in Fig. 5.11. The errors and the corresponding orders of convergence are displayed in Table 5.10.

Example 5.5(c). Consider the generalized Black–Scholes Eq. (2.9) for portfolio of options with butterfly spread delta function as the final condition with $\hat{\sigma}(S,t) = 0.4$, $\hat{r}(S,t) = 0.1+0.02\sin(10T(T-t))$, $\hat{D}(S,t) = 0.06S/S_{max}$, $T=1$, $K=5$, $S1=4$, $S2=$

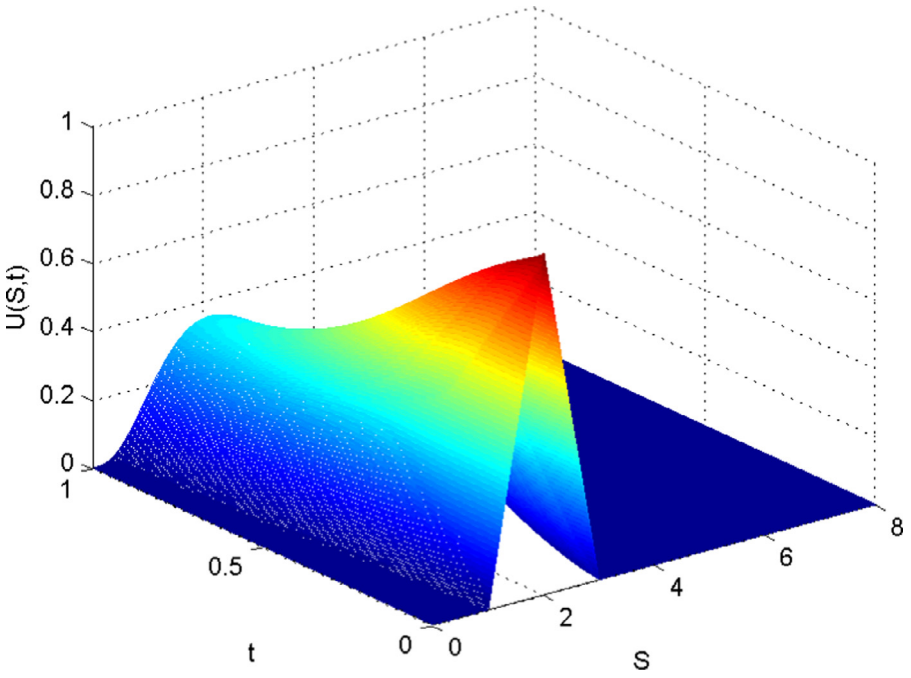

Fig. 5.9. Numerical solution of Example 5.4(b).

Table 5.11
Maximum absolute error ($E_{\max}$), root mean square error (E_{rms}) and corresponding orders of convergence $p_{\max}$ and p_{rms} for Example 5.5(c).

M	10	10×2	10×2^2	10×2^3	10×2^4	10×2^5	10×2^6
N	5	5×2	5×2^2	5×2^3	5×2^4	5×2^5	5×2^6
$E_{\max}$		4.7789e−03	1.6327e−03	3.5093e−04	8.8375e−05	2.2060e−05	5.5274e−06
$p_{\max}$			1.5494	2.2180	1.9895	2.0022	1.9968
E_{rms}		2.7326e−03	7.2859e−04	1.7301e−04	4.3184e−05	1.0834e−05	2.7156e−06
p_{rms}			1.9071	2.0743	2.0023	1.9950	1.9962

Table 5.12
Orders of convergence $\hat{p}_{\max}$ and $\hat{p}_{\text{rms}}$ for Example 5.1(a) for different values of ϵ.

$\epsilon = 10^{-j}$	$M\rightarrow$	2^4	2^5	2^6	2^7	2^8	2^9	2^{10}
$\downarrow$	$N\rightarrow$	10	10×2	10×2^2	10×2^3	10×2^4	10×2^5	10×2^6
$j=3$	$\hat{p}_{\max}$		2.1980	2.0793	1.9972	2.0263	2.0502	2.1091
4	$\hat{p}_{\max}$		2.1949	2.0744	1.9852	2.0031	2.0038	2.0089
5	$\hat{p}_{\max}$		2.1946	2.0740	1.9840	2.0008	1.9994	1.9998
6	$\hat{p}_{\max}$		2.1946	2.0739	1.9839	2.0006	1.9989	1.9989
7	$\hat{p}_{\max}$		2.1946	2.0739	1.9839	2.0006	1.9989	1.9988
⋮	⋮		⋮	⋮	⋮	⋮	⋮	⋮
10	$\hat{p}_{\max}$		2.1946	2.0739	1.9839	2.0006	1.9989	1.9988
$j=3$	$\hat{p}_{\text{rms}}$		2.1907	2.0227	2.0118	2.0263	2.0593	2.1286
4	$\hat{p}_{\text{rms}}$		2.1871	2.0160	1.9984	1.9991	2.0034	2.0105
5	$\hat{p}_{\text{rms}}$		2.1867	2.0154	1.9971	1.9964	1.9981	1.9998
6	$\hat{p}_{\text{rms}}$		2.1867	2.0153	1.9970	1.9962	1.9975	1.9987
7	$\hat{p}_{\text{rms}}$		2.1867	2.0153	1.9969	1.9962	1.9975	1.9986
⋮	⋮		⋮	⋮	⋮	⋮	⋮	⋮
10	$\hat{p}_{\text{rms}}$		2.1867	2.0153	1.9969	1.9962	1.9975	1.9986

5 and $S3 = 6$. Take $S_{max} = 10$ and $\epsilon = 10^{-6}$. The numerical solution obtained using the scheme (3.1) is depicted in Fig. 5.12. The errors and the corresponding orders of convergence are displayed in Table 5.11.

To see the influence of ϵ on the rate of convergence, some numerical experiments are conducted on the Examples 5.1(a) and 5.2(a) for different values of ϵ, and the results are shown in the Tables 5.12 and 5.13, respectively. One can observe from these tables that the order of convergence is ϵ-uniform as $\epsilon \rightarrow 0^+$.

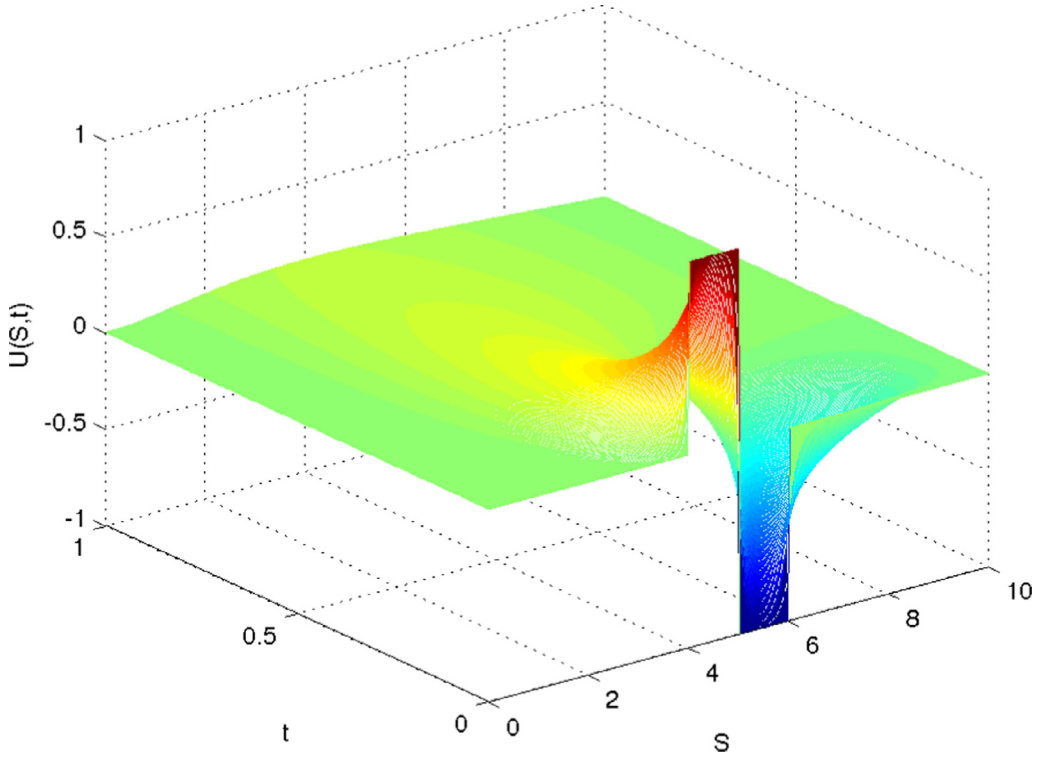

Fig. 5.10. Numerical solution of Example 5.5(a).

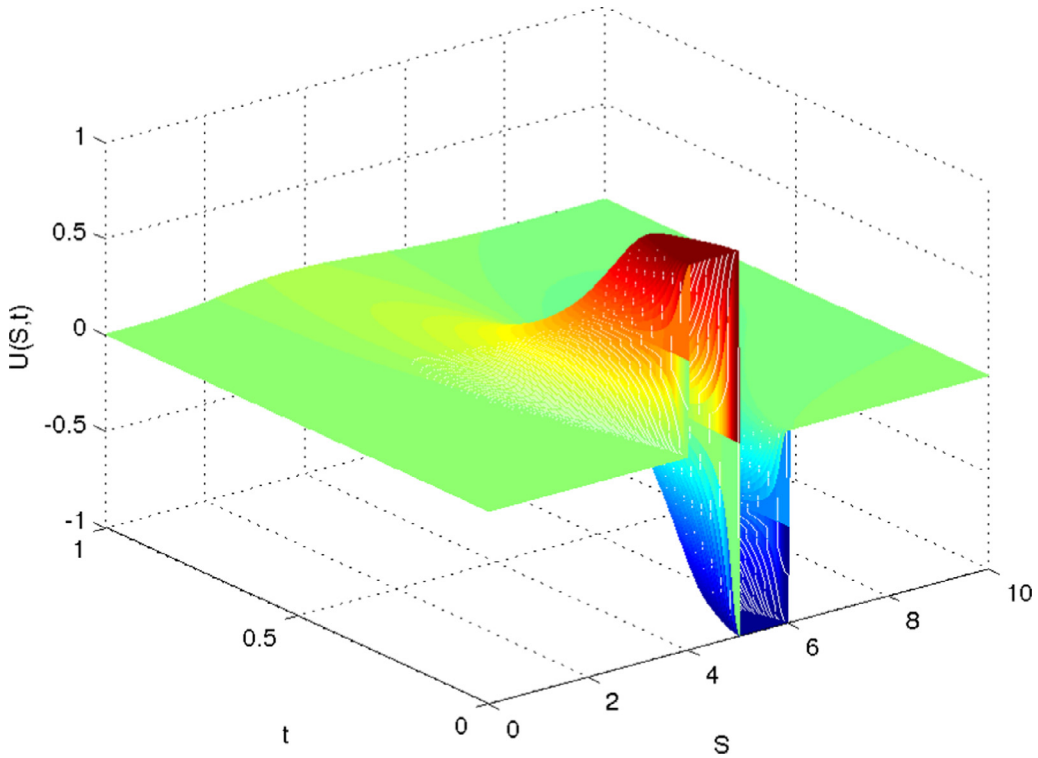

Fig. 5.11. Numerical solution of Example 5.5(b).

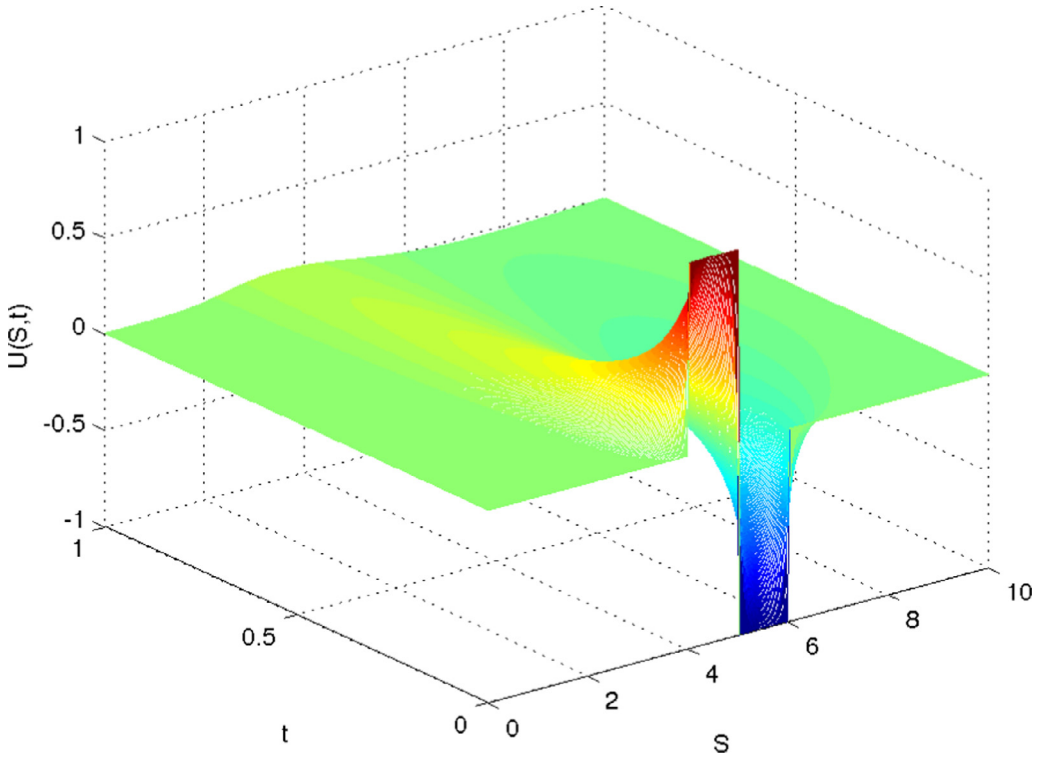

Fig. 5.12. Numerical solution of Example 5.5(c).

Table 5.13
Orders of convergence $p_{\max}$ and p_{rms} for Example 5.2(a) for different values of ϵ.

$\epsilon = 10^{-j}$ ↓	$M \rightarrow$ $N \rightarrow$	2^4 10	2^5 10×2	2^6 10×2^2	2^7 10×2^3	2^8 10×2^4
$j = 3$	$p_{\max}$		1.8951	2.4882	1.9717	1.9811
4	$p_{\max}$		1.8957	2.4866	1.9695	1.9780
5	$p_{\max}$		1.8957	2.4864	1.9693	1.9777
6	$p_{\max}$		1.8957	2.4864	1.9693	1.9777
7	$p_{\max}$		1.8957	2.4864	1.9693	1.9777
⋮	⋮		⋮	⋮	⋮	⋮
10	$p_{\max}$		1.8957	2.4864	1.9693	1.9777
$j = 3$	p_{rms}		2.2124	2.2381	1.9753	2.0047
4	p_{rms}		2.2116	2.2344	1.9697	1.9932
5	p_{rms}		2.2115	2.2340	1.9692	1.9920
6	p_{rms}		2.2115	2.2340	1.9691	1.9919
7	p_{rms}		2.2115	2.2340	1.9691	1.9919
⋮	⋮		⋮	⋮	⋮	⋮
10	p_{rms}		2.2115	2.2340	1.9691	1.9919

This paper numerically solves the generalized form of Black–Scholes equation in its almost original form which is degenerate but forward in time, using the HODIE scheme in the space direction and the two-step backward differentiation formula for discretization in the time direction and gives second order convergence in space as well as time direction. In [10], the scheme was developed for solving the generalized form of Black–Scholes equation. But the problem needs to be first transformed to non-degenerate parabolic partial differential equation and then it is solved numerically. Also the scheme in [10] constitutes of obtaining semi-discrete scheme first (by semi-discretization in time only) and then the complete discrete scheme (by doing spatial discretization also) which results in convergence analysis at both the steps. Our analysis is much simpler as it avoids the convergence analysis at the semi-discrete step. Clavero et al. emphasized on such competence of the simultaneous discretization in their work [25]. In [10], Rannacher time stepping is required to remove the spurious oscillations near the singularities, produced by applying Crank-Nicolson scheme for temporal discretization. In the present work two-step backward differentiation method is used to achieve second order accuracy in time direction without any oscillations. In [20], a finite difference scheme was developed for generalized Black–Scholes equation but they considered

a non-dividend paying market, the interest rate was function of only time variable and the scheme had only first order convergence in time. Also the risk free interest rate in their test problems were taken to be constant.

In [21] and [22], fitted finite volume method was used for numerically solving generalized Black–Scholes equation. The dividend was taken to be function of stock price and time but the volatility and the risk free interest rate were taken to be functions of time only. Moreover in the numerical experiments, volatility was assumed to be some constant and dividend was taken as function of stock price only. However in the present work, σ, r and D are all taken to be functions of space and time variables for proving theoretical results, as well as in numerical examples. Using our scheme one can get second order accuracy both in space and time as proved in the error analysis and is easily observable in the numerical experiments where all the parameters $\hat{\sigma}$, $\hat{r}$ and $\hat{D}$ are taken as functions of both S and t.

Acknowledgment

The authors gratefully acknowledge the valuable comments and suggestions from the anonymous referees. The second author would like to thank National Board for Higher Mathematics, DAE (Government of India) for financial support in form of research grant.

References

[1] M. Capiński, T. Zastawniak, Mathematics for Finance: An Introduction to Financial Engineering, Springer-Verlag London, Ltd., London, 2003.
[2] P. Wilmott, J. Dewynne, S. Howison, Option Pricing: Mathematical Models and computation, Oxford Financial, 1998.
[3] F. Black, M. Scholes, The pricing of options and corporate liabilities, J. Polit. Econ. 81 (1973) 637–654.
[4] J. Zhao, M. Davison, R.M. Corless, Compact finite difference method for American option pricing, J. Comput. Appl. Math. 206 (2007) 306–321.
[5] R.C. Merton, Theory of rational option pricing, Bell J. Econ. Manag. Sci. 4 (1973) 141–183.
[6] J.C. Cox, S.A. Ross, M. Rubinstein, Option pricing: a simplified approach, J. Financ. Econ. 7 (1979) 229–263.
[7] M. Parkinson, Option pricing: the American put, J. Bus. 50 (1977) 21–36.
[8] J. Hull, A. White, The use of the control variate technique in option pricing, J. Financ. Quant. Anal. 23 (1988) 237–251.
[9] R. Geske, K. Shastri, Valuation by approximation: a comparison of alternative option valuation techniques, J. Financ. Quant. Anal. 20 (1985) 45–71.
[10] M.K. Kadalbajoo, L.P. Tripathi, A. Kumar, A cubic B-spline collocation method for a numerical solution of the generalized Black–Scholes equation, Math. Comput. Model. 55 (2012) 1483–1505.
[11] H. Han, X. Wu, A fast numerical method for the Black-Scholes equation of American options, SIAM J. Numer. Anal. 41 (2004) 2081–2095.
[12] J. Zhao, R.M. Corless, M. Davison, Financial applications of symbolically generated compact finite difference formulae, in: Symbolic-Numeric Computation, Birkhäuser, Basel, 2007, pp. 361–374. Trends Mathematics
[13] D.Y. Tangman, A. Gopaul, M. Bhuruth, Numerical pricing of options using high-order compact finite difference schemes, J. Comput. Appl. Math. 218 (2008) 270–280.
[14] H.-J. Bungartz, A. Heinecke, D. Pflüger, S. Schraufstetter, Option pricing with a direct adaptive sparse grid approach, J. Comput. Appl. Math. 236 (2012) 3741–3750.
[15] A. Andalaft-Chacur, M.M. Ali, J. González Salazar, Real options pricing by the finite element method, Comput. Math. Appl. 61 (2011) 2863–2873.
[16] B. Düring, M. Fournié, A. Jüngel, Convergence of a high-order compact finite difference scheme for a nonlinear Black–Scholes equation, M2AN Math. Model. Numer. Anal. 38 (2004) 359–369.
[17] S.-P. Zhu, A. Badran, X. Lu, A new exact solution for pricing European options in a two-state regime-switching economy, Comput. Math. Appl. 64 (2012) 2744–2755.
[18] G.W. Buetow, J.S. Sochacki, The trade-offs between alternative finite difference techniques used to price derivative securities, Appl. Math. Comput. 115 (2000) 177–190.
[19] J. Ankudinova, M. Ehrhardt, On the numerical solution of nonlinear Black–Scholes equations, Comput. Math. Appl. 56 (2008) 799–812.
[20] Z. Cen, A. Le, A robust and accurate finite difference method for a generalized Black-Scholes equation, J. Comput. Appl. Math. 235 (2011) 3728–3733.
[21] S. Wang, A novel fitted finite volume method for the Black–Scholes equation governing option pricing, IMA J. Numer. Anal. 24 (2004) 699–720.
[22] R. Valkov, Fitted finite volume method for a generalized Black–Scholes equation transformed on finite interval, Numer. Algorithms 65 (2014) 195–220.
[23] S. Wang, S. Zhang, Z. Fang, A superconvergent fitted finite volume method for Block–Scholes equations governing European and American option valuation, Numer. Methods Partial Differ. Eq. 31 (2015) 1190–1208.
[24] R.E. Lynch, J.R. Rice, A high-order difference method for differential equations, Math. Comput. 34 (1980) 333–372.
[25] C. Clavero, J.L. Gracia, M. Stynes, A simpler analysis of a hybrid numerical method for time-dependent convection-diffusion problems, J. Comput. Appl. Math. 235 (2011) 5240–5248.
[26] S. Kumar, S.C.S. Rao, A robust overlapping Schwarz domain decomposition algorithm for time-dependent singularly perturbed reaction-diffusion problems, J. Comput. Appl. Math. 261 (2014) 127–138.
[27] A. Friedman, Partial Differential Equations of Parabolic Type, Prentice-Hall, Inc., 1964. Englewood Cliffs, N.J.
[28] S. Heston, G. Zhou, On the rate of convergence of discrete-time contingent claims, Math. Finance 10 (2000) 53–75.
[29] D.M. Pooley, K.R. Vetzal, P.A. Forsyth, Convergence remedies for non-smooth payoffs in option pricing, J. Comput. Finance 6 (2003) 25–40.
[30] O.A. Ladyženskaja, V.A. Solonnikov, N.N. Ural′ceva, Linear and Quasilinear Equations of Parabolic Type, American Mathematical Society, Providence, RI, 1968. Transl. 23.
[31] C. Cho, T. Kim, Y. Kwon, Estimation of local volatilities in a generalized Black-Scholes model, Appl. Math. Comput. 162 (2005) 1135–1149.
[32] C. Vázquez, An upwind numerical approach for an American and European option pricing model, Appl. Math. Comput. 97 (1998) 273–286.
[33] R. Kangro, R. Nicolaides, Far field boundary conditions for Black–Scholes equations, SIAM J. Numer. Anal. 38 (2000) 1357–1368.
[34] C. Clavero, J.L. Gracia, F. Lisbona, High order methods on Shishkin meshes for singular perturbation problems of convection-diffusion type, Numer. Algorithms 22 (1999) 73–97.
[35] R.B. Kellogg, A. Tsan, Analysis of some difference approximations for a singular perturbation problem without turning points, Math. Comp. 32 (1978) 1025–1039.
[36] R.S. Varga, Matrix Iterative Analysis, Springer-Verlag, Berlin, 2000.
[37] R.J. LeVeque, Finite Difference Methods for Ordinary and Partial Differential Equations, Society for Industrial and Applied Mathematics (SIAM), Philadelphia, PA, 2007.